ASME Journal of Tribology
Online journal at:
https://asmedigitalcollection.asme.org/tribology

Tribology and Tribocorrosion of Case-Hardened Steels: A Review

Q1

Tomas Grejtak[1]
Materials Science and Technology Division,
Oak Ridge National Laboratory,
Oak Ridge, TN 37831
e-mail: grejtakt@ornl.gov

Wenbo Wang
Materials Science and Technology Division,
Oak Ridge National Laboratory,
Oak Ridge, TN 37831
e-mail: wangw2@ornl.gov

Jun Qu[1]
Materials Science and Technology Division,
Oak Ridge National Laboratory,
Oak Ridge, TN 37831
e-mail: qujn@ornl.gov

This report reviews the tribological and tribocorrosion performance of steels that are case-hardened via boriding, chromizing, carburizing, nitriding, nitrocarburizing, and carbonitriding. Case-hardening is commonly used to improve the hardness, impact durability, wear resistance, and corrosion resistance of steel alloys and has been successfully applied in various industries, providing a cost-effective, high-throughput solution for applications involving contact and sliding interfaces in complex service environments. This article summarizes the literature results of the wear and friction behavior of common case-hardening methods for steel alloys under various conditions, including corrosive environments. Special attention is given to the influences of case-hardening process parameters and alloy composition on tribological performance. By discussing key findings from the literature, this review provides insights into optimizing case-hardening processes for improving the tribological and tribocorrosion performance of steel alloys.
[DOI: 10.1115/1.4069243]

Keywords: case-hardening, steel, wear, tribocorrosion, surface properties, surface characterization, wear mechanisms, corrosion, surface layers, surface properties and characterization, surface treatments

Q2

1 Introduction

Modern engineering applications demand materials that exhibit high surface hardness, wear resistance, and a tough and ductile core. Steels with various heat treatments are broadly used because of their combined high strength and toughness. However, further increasing hardness, strength, and wear resistance via traditional hardening processes can significantly reduce the fracture toughness of the bulk material and introduce substantial residual stresses, particularly in large components. As a result, such components become more susceptible to failure under shocks or repetitive impact, conditions commonly encountered by gears, shafts, and rails. To address these challenges, case-hardening techniques have been extensively adopted. Case-hardening, also known as surface hardening, is a metallurgical process that enhances the hardness, wear resistance, and impact durability of metals by selectively hardening their outer surface layer [1–3]. Beyond improving the mechanical properties of the surface layer, case-hardening can also enhance corrosion resistance [4–8]. The combination of these properties achieved through case-hardening is critical for demanding applications in the automotive [9–11], aerospace [12,13], and tooling [14,15] industries.

Case-hardening is achieved by modifying the composition and microstructure of a metal surface via thermochemical diffusion [1–3]. In this process, the metal is exposed to a solid, gaseous, or liquid medium containing the hardening element. The absorbed atoms then diffuse into the surface and react with iron and other substrate elements to form a case-hardened layer that is only tens to hundreds of micrometers thick, preserving the properties and microstructure of the core. Depending on the case-hardening medium, the most common methods are carburizing [16–18], boriding [19], nitriding [16], carbonitriding [18,20], nitrocarburizing [21,22], and chromizing [23,24]. The selection of a case-hardening method depends on several factors, including composition and properties of the substrate; requirements for hardness, toughness, wear resistance, and corrosion resistance; and application-specific demands or operating conditions. Based on these criteria, different case-hardening methods are suited to different steel types and performance requirements. Carburizing is typically applied to low-carbon steels to increase their surface hardness and wear resistance [16,18,25]. Carbonitriding, while similar to carburizing, provides slightly higher surface hardness [18]. Boriding provides very high hardness along with excellent wear resistance and corrosion resistance and is applied to a broader range of steel materials [19]. Chromizing also enhances wear resistance and corrosion resistance but offers lower hardness than boriding and is not suitable for high-alloy steels [23,24]. Nitriding, performed at relatively lower temperatures, is particularly effective for alloy steel and stainless steel, providing high surface hardness, wear resistance, and good corrosion resistance [16,21]. Nitrocarburizing, another lower temperature process, yields lower hardness, wear resistance, and corrosion resistance than nitriding but is suitable for both carbon and alloy steels [21].

This article provides a review of the tribological and tribocorrosion performance of case-hardened steel alloys. The fundamentals of each case-hardening technique are described first, followed by an analysis of the tribological and tribocorrosion performance in correlation with the case-hardening process parameters, steel composition, and test conditions.

[1]Corresponding authors.

Contributed by the Tribology Division of ASME for publication in the Journal of Tribology. Manuscript received April 7, 2025; final manuscript received July 18, 2025; published online xx xx, xxxx. Assoc. Editor: Kora Farokhzadeh.

2 Case-Hardening Mechanisms

Briefly, case-hardening is a diffusion-based thermomechanical process in which atoms from the case-hardening medium penetrate the metal surface [1–3], as shown in Fig. 1 [26]. This diffusion is driven by a concentration gradient, causing atoms to migrate from a region of higher concentration (solid, gas, liquid) to a region of lower concentration (substrate). The diffusion rate depends on several factors, including temperature, time, substrate composition, and compound concentration. Specifically, higher temperatures increase atomic mobility, which accelerates diffusion [1], while longer process durations result in greater diffusion depths. Similarly, increasing the concentration of the diffusing compound enhances the diffusion rate. However, the presence of alloying elements such as molybdenum, vanadium, or chromium can inhibit diffusion and thus reduce the thickness of the case [19,27]. On the other hand, these alloying elements can promote the formation of hard carbides that improve the surface hardness of the case-hardened layer. The resultant case-hardened layer exhibits a gradient in composition from a compound-rich outer surface to an iron-dominant inner core. The composition gradient typically produces a corresponding hardness gradient throughout the layer [27–29]. The microstructure of the case-hardened layer depends on the compound composition and the steel substrate. It can consist of single or dual phases, often with carbide formation owing to the presence of alloying elements in the substrate [19,23,24]. Optimization of process parameters is essential to control the morphology and achieve the desired properties of the case-hardened layer.

3 Tribological and Tribocorrosion Behavior of Case-Hardened Steels

To achieve the desired performance, multiple factors must be considered when selecting an appropriate case-hardening method, particularly for optimizing tribological performance. Case-hardening is widely used to improve the wear resistance of steel materials in applications involving sliding interfaces [3,11,12,30]. While it may seem intuitive that increasing the hardness would improve the wear resistance, tribological properties are not inherent material properties. Instead, they are strongly dependent on the test conditions, including contact pressure, environment (e.g., dry, lubricated, inert, humid, high or low temperature, corrosive), counter-body materials, and other factors [31,32]. Therefore, selecting a case-hardening method that aligns with specific operational conditions is crucial for minimizing wear and ensuring reliable long-term performance. Additionally, different steel materials possess distinct properties, and selecting an appropriate case-hardening method is essential to tailor surface characteristics that meet specific performance requirements for a given application. For example, stainless steels generally offer excellent corrosion resistance but are often limited in tribological applications due to their relatively low surface hardness and poor wear performance [33]. In contrast, tool steels typically possess greater surface hardness and wear resistance than stainless steels primarily due to their higher carbon content and the presence of carbide-forming precipitates [34]. However, tool steels might be susceptible to corrosion due to micro-galvanic coupling between the matrix and precipitates [34]. When external stress or wear acts synergistically with corrosive environments, steel alloys can experience tribocorrosion—a degradation process that accelerates material loss beyond what would occur from wear or corrosion alone. The following review and discussion of the tribological and tribocorrosion behavior of various case-hardening methods in this section provide valuable insights for optimizing these processes to enhance the surface durability of steel components in demanding service conditions.

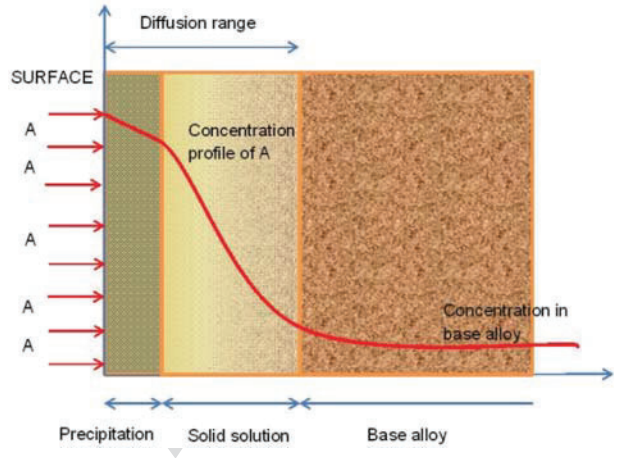

Q18 **Fig. 1 Schematic representation of thermochemical treatment of an alloy showing distribution of a case-hardening medium A into the alloy surface. Reproduced from Ref. [26].**

3.1 Carburizing.

Carburizing is primarily applied to low-carbon steels, but it can also be applied to low-alloy steels to enhance surface hardness and wear resistance by diffusing carbon atoms into the surface at temperatures up to about 1000 °C [18]. The advantage of carburizing is that it enables low-carbon ferrous alloys to achieve a hard surface while maintaining adequate toughness and ductility in the core. Low-carbon steels with carbon content up to 0.3% are softer and more ductile and cannot be effectively hardened through conventional heat treatment due to insufficient carbon. Instead, these alloys are hardened via carburizing, which typically increases the carbon content in the surface layer to approximately 0.8–1% [18]. Following carburizing, these components are typically quenched to form a hard martensitic surface. This surface may also contain retained austenite, bainite, or pearlite [35]. Carburizing stainless steel is challenging due to its higher chromium content, which significantly retards carbon diffusion. However, one of the main advantages of carburizing over other case-hardening methods is its ability to produce a relatively thick hardened layer that can be up to 1.5 mm thick [36]. The thickness of the carburized layer depends on the process parameters, as shown in Fig. 2 [37]. The hardness of the carburized layer can reach up to approximately 950 HV [18], which is generally lower than the hardness achieved by boriding, nitriding, or chromizing. Low-carbon ferrous alloys can be carburized via powder-pack cementation, gas, plasma, vacuum, or salt-bath carburizing [18].

Most of the reviewed studies focused on tribological characterization of carburized low-carbon and low-alloy steels for which carburizing is most beneficial. The reviewed literature is summarized in Table 1. In most of the reviewed work, carburizing was accomplished via the gas-carburizing method. Carbon concentration can affect the case thickness, hardness, and wear resistance. In vacuum carburizing, carbon concentration can be optimized by controlling the boost-to-diffusion ratio. In the boost stage, the steel substrate is exposed to a high-carbon potential atmosphere to enrich the surface with carbon, followed by the diffusion stage, during which a lower-carbon or inert gas atmosphere allows carbon to diffuse deeper into the steel. Lowering the boost-to-diffusion ratio to the level of 20–30% in vacuum carburizing of 23CrNi3MoA gear steel led to a lower concentration of carbon but a deeper case, which consequently reduced wear and friction, as shown in Fig. 3 [38]. At lower boost-to-diffusion ratios, retained austenite size is smaller and more uniformly distributed, which contributed to improved tribological performance. However, when the boost-to-diffusion ratio ranged between 30 and 50%, severe abrasive wear was observed due to reduced hardness. Another study investigated the effect of the carbon concentration in gas-carburized American Iron and Steel Institute (AISI) 8620 gear steel by varying the carbon potential from 0.45% to 1.05%. The results showed that higher hardness and higher amount of retained austenite led to better wear resistance [39]. Friction was unaffected by the carburizing

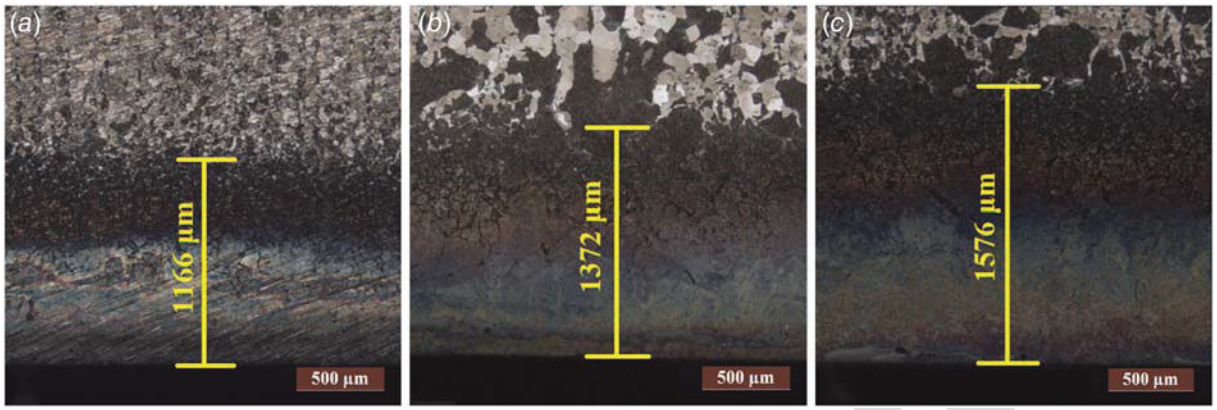

Fig. 2 Optical images of a low-alloy gear steel carburized for (*a*) 4 h, (*b*) 6 h, and (*c*) 8 h at 920 °C. The thickness of the carburized layer increases by 41% from 4 h to 8 h of processing time. Reproduced from Ref. [37]. Copyright by IOP Publishing.

treatment, with performance comparable to that of the untreated base.

In a study reported by Shi et al. [42], vacuum carburizing with one to four cycles was conducted on 17CrNiMo6 gear steel in dry and oil-lubricated conditions at room temperature (RT) and 100 °C. The study showed that increasing the number of carburizing cycles led to a thicker hardened layer and a greater number and size of carbides, resulting in higher surface hardness. However, the tribological performance showed mixed trends. In dry sliding conditions, the lowest wear occurred after one cycle, whereas three cycles resulted in the highest wear but also the lowest friction. In contrast, under oil-lubricated sliding, the lowest friction was observed after a single cycle. At an elevated temperature of 100 °C, friction measurements in both dry and lubricated

Table 1 Summary of the literature on tribological and tribocorrosion studies of carburized steels

Steel material	Case-hardening conditions	Hardness	Wear test method	Observations	Ref.
23CrNi3MoA	Vacuum: 930 °C, varying boost diffusion ratio	660–720 HV	Ball-on-disc *Counter-body*: WC-Co	Lower wear, friction, and higher hardness were achieved with a lower boost-to-diffusion ratio, due to lower-carbon concentration. Lower content of retained austenite (RA) 20–30%, enhanced mechanical stability.	[38]
AISI 8620	Gas: 925 °C, 4 h, varying carbon potential	3–9 GPa	Ball-on-flat *Counter-body*: diamond	Higher carbon potential resulted in higher hardness and increased carbon concentration near the surface, which also led to a higher RA% and higher wear resistance.	[39]
AISI 8620	Gas: 925 °C, 320 and 660 min	840 HV	Ball-on-disc *Counter-body*: abrasive paper	Longer process time resulted in a thicker layer, higher hardness, and wear.	[29]
20CrMnTi and 20CrMnMoNi	Gas: 930 °C	750 HV	Ring-on-disc *Counter-body*: AISI 52100	Carburized 20CrMnMoNi formed a bainitic microstructure, which improved the wear resistance. Carburized 20CrMnTi formed a martensitic microstructure with subsurface cracks.	[40]
20CrMnTi	Gas: 930 °C, 210 min	750 HV	Ball-on-disc fretting *Counter-body*: C45	Compared to virgin and quenched, carburized 20CrMnTi had higher hardness, lower wear, and friction. Abrasive, adhesive, and oxidative wear.	[41]
17CrNiMo6	Vacuum: 980 °C, 8 h	867 HV	Ball-on-disc *Counter-body*: abrasive paper RT dry and oil lubrication, 100 °C	Thickness and hardness increased with cycling RT dry: 1 cycle—lowest wear, abrasive, three cycles lowest friction but highest wear due to excessive coarsening of carbides. RT oil: 1 cycle—lowest friction 100 °C oil: no change in friction but higher oxidation	[42]
AISI 8620	Vacuum: 900 °C, 3 h	65 HRC	Ball-on-disc *Counter-body*: EN31 100 °C	Adhesive and plowing wear.	[43]
316L	Plasma: 470 °C, 15 h	900 HV	Pin-on-disc *Counter-body*: Al_2O_3 *Solution*: 1 M H_2SO_4	Carburizing significantly improved the tribocorrosion resistance at anodic potentials by up to 10 times. At cathodic potentials, its effectiveness was limited due to third-body abrasive wear.	[44][a]
316L	Plasma: 470 °C, 15 h	870 HV	Ball-on-disc *Counter-body*: Al_2O_3 *Solution*: 0.5 M H_2SO_4	Carburized layer enhanced the tribocorrosion resistance of 316L stainless steel by 40% due to combined high resistance to wear and great passivity to resist corrosion.	[45][a]
AISI 420	Plasma: 450 °C, 8 and 12 h	1250 HV	Erosion test *Counter-body*: quartz powder *Solution*: 3.5% NaCl	Carburized layer provided better resistance to tribocorrosion, which improved with process time due to a thicker cementite layer and better repassivation behavior.	[46][a]

[a]Tribocorrosion studies.

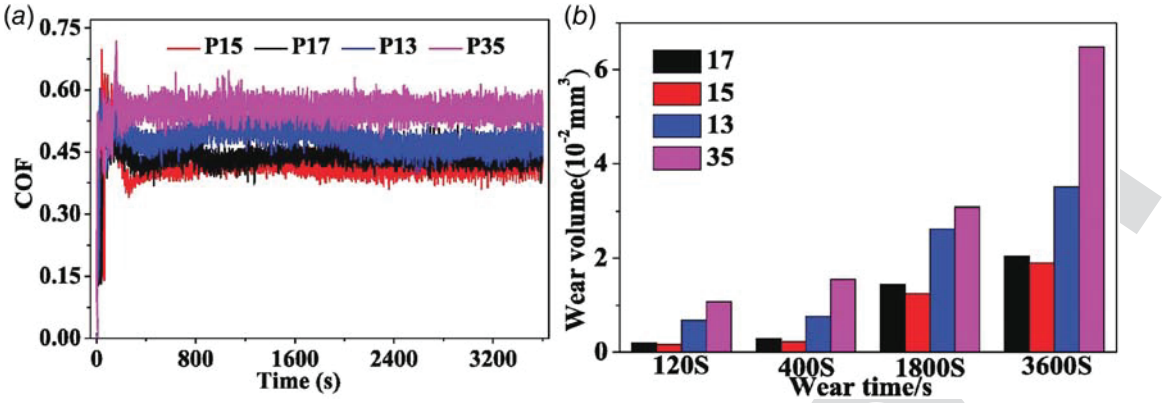

Fig. 3 Effect of boost-to-diffusion ratio and sliding duration on (*a*) coefficient of friction (COF) and (*b*) wear volume of vacuum-carburized 23CrNi3MoA steel. Note: 15 means boost-to-diffusion ratio of 1:5, etc. Reproduced from Ref. [38]. Copyright 2022 by Elsevier.

sliding conditions showed no clear dependence on the number of carburizing cycles. The dominant wear mechanisms were abrasive and oxidative, with minor contributions from adhesive wear.

The influence of process duration on tribological properties was demonstrated on gas-carburized AISI 8620 steel [29]. A carburizing time of 660 min resulted in higher hardness and wear resistance compared with a 320-min carburizing time. The improvement in hardness and wear resistance was attributed to a deeper carburized case, which increased with process time.

To investigate the influence of the base microstructure on the tribological behavior, 20CrMnTi with martensitic microstructure and 20CrMnMoTi with bainitic microstructure were gas-carburized and evaluated [40]. The study concluded that the bainitic microstructure exhibited superior wear resistance, which was attributed to its high strength and toughness, the presence of carbon-enriched film-like austenite that inhibits crack propagation, and an extremely fine α-phase that enhances hardness. In another study, fretting wear tests on gas-carburized 20CrMnTi gear steel showed that the dominant wear mode at lower contact load is abrasion, whereas adhesive and oxidative wear are dominant at higher contact loads [41].

Sun and Bailey [45] studied the tribocorrosion behavior of low-temperature carburized stainless steel in 0.5 M H_2SO_4 solution. In tribocorrosion tests conducted under open circuit potential conditions, the carburized layer enhanced the tribocorrosion resistance of 316L stainless steel by 40% due to its combined high resistance to mechanical wear and excellent corrosion passivity. In another study, plasma-carburized 316L stainless steel was used to investigate the effect of electrochemical potential on tribocorrosion performance [44]. Carburizing significantly improved the tribocorrosion resistance at anodic potentials by up to 10 times under the designed test protocols in 1 M H_2SO_4 solution. The carburized layer also improved the wear resistance of 316L stainless steel at cathodic potentials; however, its effectiveness was limited by third-body abrasive wear.

Mainardi et al. [46] investigated the effect of low-temperature plasma carburizing on the synergetic interaction between erosion and corrosion of AISI 420 martensitic stainless steel exposed to a 3.5% NaCl solution. Carburizing improved both corrosion–erosion synergy and overall corrosion resistance. Notably, the 12-h treatment outperformed the 8-h treatment by forming a thicker cementite layer and demonstrating improved repassivation behavior during tribocorrosion, attributed to the introduction of interstitial carbon.

The passivation mechanism of a carburized layer of AISI 316L stainless steel was discussed in Ref. [47]. The formation and transport of oxygen vacancies at the metal/passive film interface are critical for passive film growth. However, a high near-surface carbon concentration hinders the oxygen vacancy formation and Cr migration due to strong Cr–C bonding and the presence of a C-rich layer at the oxide/metal interface. This impedes the film growth compared with the untreated steel. Nevertheless, long-term immersion tests indicated that the passive film on the carburized steel surface continued to grow over time, with a decreasing corrosion rate. Even in the presence of surface defects, no evidence of galvanic coupling was observed between the exposed carburized layer and the underlying alloy core.

The downside of carburizing is that the high-temperature process can cause austenite grain coarsening and particle redissolution in the substrate beneath the carburized zone [48,49], which could aggravate the mechanical properties. A study on carburized 20CrMnTi gear steel showed that the austenite grain coarsening is due to rapid dissolution of (Ti,Mo) (C, N) precipitates, which is accelerated with a higher carburizing temperature up to 980 °C, leading to a faster austenite grain growth [48]. Austenite grain coarsening was also shown in the carburized 16MnCr5 steel at 920 °C; however, it was demonstrated that the grain coarsening can be minimized with prenitriding [49].

In all studies, carburizing improved hardness as well as wear resistance and tribocorrosion resistance compared with the steel base. In general, the thickness of the carburized layer increases with increasing carburizing time and temperature. Extended process times enhance the uniformity and thickness of the carburized layer. However, the studies investigating the effect of carbon concentration showed contradictory results. Carbon concentration affects the amount and size of retained austenite, and studies have demonstrated that a higher volume fraction positively affects the wear and hardness. More studies need to be conducted to determine the effect of carbon concentration, composition, and microstructure of the carburized layer on the tribological behavior. Abrasive wear is the dominant wear mode in the carburized ferrous alloys. Other identified wear modes were oxidative and adhesive. By contrast, the carburized layer exhibits good repassivation and surface protection during tribocorrosion testing. As reported for stainless steels [47], a high-carbon concentration in the carburized layer can slow down the passive film formation. Still, the passive film continues to grow over time, consequently reducing corrosion and the risk of galvanic coupling under tribocorrosion conditions. It is important to carefully control the processing conditions to avoid the formation of detrimental precipitates, such as chromium-rich carbides, which can deplete chromium from the matrix, leading to significantly reduced corrosion resistance.

3.2 Boriding. Boriding, or boronizing, is used to increase hardness, wear resistance, and corrosion resistance of metals [19,50]. Boriding surface treatment offers several advantages over other conventional case-hardening methods. It can be applied to a wide range of steel materials. Unlike carburizing, nitriding, or chromizing. A borided layer can achieve extremely high hardness values, reaching up to approximately 3300 HV [19]. The

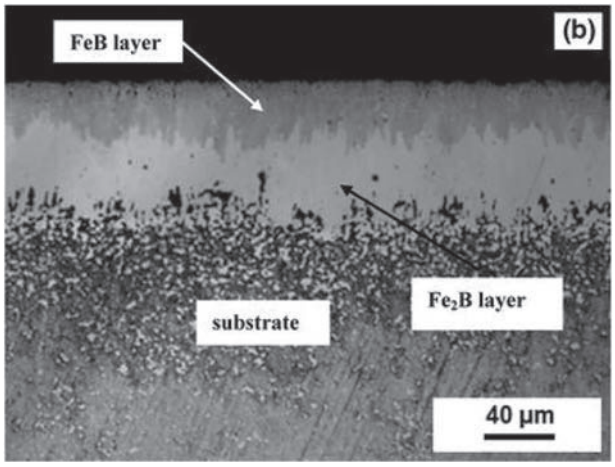

Fig. 4 Cross section of borided AISI M2 steel showing a bilayer composed of FeB and Fe_2B formed at 1050 °C for 6 h. Reproduced from Ref. [52]. Copyright 2011 by Springer Nature.

exceptional hardness of borided surfaces results in their high wear resistance. Unlike carburizing and nitriding, boriding requires higher processing temperatures, which can be in the range of 800–1000 °C [19]. The borided layer could be either a single-phased Fe_2B or double-phased Fe_2B and FeB [19,51,52], as shown in Fig. 4 [52] and up to 250 μm thick [19]. Ferrous metals can be borided by several methods, such as powder-pack cementation [19,53,54], paste [55], plasma [19], or fluidized-bed boriding [19].

Literature on tribological and tribocorrosion characterization of borided steel materials is summarized in Table 2. Most studies have focused on tribological characterization of borided steel materials made by powder-pack boriding because this technique is the most widely used in the industry [19]. Several studies found that increasing process time and temperature improved the tribological performance. Tribological characterization of borided AISI H13 tool steel at process temperatures of 800–1000 °C for 2–6 h showed that increasing process temperature and time increased the hardness of the borided layer, thereby improving wear resistance [56]. Higher temperatures led to the formation of a harder FeB phase, in addition to the Fe_2B phase that formed in all process conditions, contributing to increased overall hardness and wear resistance.

Similar trends were found with a micro-abrasion wear testing of borided H13 tool steel, revealing that abrasive wear resistance increased with process temperature from 578 to 634 °C owing to increased hardness and thickness of the borided layer [57].

A positive correlation between wear resistance and the thickness of the borided layer was also found in borided D2 tool steel [58]. Increasing process temperature from 900 to 1000 °C for 3, 5, and 7 h resulted in a thicker borided layer and, on average, higher hardness. A thicker borided layer at longer process times and higher temperatures improved wear resistance: the 1000 °C sample exhibited polishing wear owing to a lower FeB/Fe_2B phase ratio, whereas the 900 °C sample showed delamination wear. However, the friction remained unaffected by processing conditions but was significantly lower than in the untreated D2 sample. Positive effects of increasing process temperatures and times on case depth and hardness were also observed in borided SAE 1020 low-carbon steel, as shown in Fig. 5 [54].

Other studies showed contradicting trends among wear performance, process temperature, and time. The study of borided high-manganese steel, processed at 850, 900, and 950 °C for 2, 4, and 6 h, showed that the thickness of the borided layer appreciably increased with process time and temperature [6]. However, the wear testing did not reveal any notable trends in the wear behavior and hardness with respect to the process temperature and time. Although all borided samples contained FeB and Fe_2B phases, their purity and morphology could have varied across the process parameters: a high content of manganese could have affected the wear resistance and hardness. In another study, tribological characterization of borided AISI 316L stainless steel showed varying trends between wear performance and process temperatures of 850, 950, and 1050 °C for 2, 4, and 6 h [59]. Although the process temperatures of 950 and 1050 °C significantly increased the thickness of the borided layer, the wear performance was inconsistent.

Boriding surface treatment has also been applied to cutting tools used in biomass comminution equipment [15]. The knife mill test demonstrated that wear on borided D2 tool steel knives was reduced by one-third compared with the untreated baseline tool steel blades. The borided knives experienced abrasion from the cutting action of biomass as well as erosion from impact with inorganic particles. In biomass comminution using a shredder, borided D2 cutters showed a tenfold lower wear rate compared to untreated D2 cutters [60].

Tribological behavior of borided steel materials prepared with methods other than powder-pack boriding has also been studied. Nora et al. [5] compared wear and friction of borided AISI 4130 low-carbon steel prepared using three methods: powder-pack boriding, nitrocarburizing, and a combination of powder-pack boriding with nitrocarburizing. The wear testing showed that the powder-pack boriding alone resulted in the highest hardness and wear resistance and lowest friction among the examined surface treatment techniques. The presence of nitrogen and carbon in the nitrocarburizing process reduced the thickness of the borided layer and decreased the hardness, leading to worse wear performance.

Another study characterized the wear and friction of 31CrMoV9 and H13 tool steels made by paste boriding at 900 °C for 4 h and 950 °C for 6 h, respectively [55]. The wear and friction performance of both borided steels was similar at RT but differed significantly at high temperatures. At 500 °C, wear and friction increased because the borided layer cracked. Wear increased by one order of magnitude in H13 tool steel and two orders of magnitude in 31CrMoV9, where a lower FeB phase content caused tensile thermal stress and promoted cracking. By contrast, the higher FeB content in H13 induced compressive stress, limiting crack propagation.

Several studies investigated wear and friction characteristics of borided metals in oil-lubricated conditions. Lubrication of powder-pack borided AISI H13 tool steel with SAE 10W-40 engine oil reduced the wear rate by 10-fold and friction by sevenfold compared with the dry test [62]. Lubrication notably reduced the surface damage, although microcracks and pitting were still observed. In another study, borided 4140 medium-carbon, low-alloy steel lubricated with the synthetic engine oil FE 5W-30 exhibited a 10-fold increase in the wear resistance and a fivefold reduction in friction compared with the dry sliding conditions [63]. This study also investigated the effect of heat treatment by comparing samples treated by boriding with samples treated by a combination of boriding and heat treatment. The additional heat-treating of the borided samples reduces the wear rate under lubricated conditions because surface pores form and absorb the lubricant and enhance lubrication. Greco et al. [61] investigated AISI 9310 gear steel treated with different methods: case carburizing, electrochemical boriding, and borocarburizing tested with a synthetic poly alpha olphaline oil and a synthetic gear oil with 1.0 wt% nanocolloidal BN particles. Electrochemical boriding and borocarburizing significantly increased the hardness and wear resistance of 9310 gear steel compared with carburizing, and nanocolloidal BN in gear oil formed a protective tribofilm, further enhancing tribological performance.

Only a few studies investigated the tribocorrosion behavior of borided steel materials. Tribological testing of powder-pack borided AISI 4140 steel in 3.5% NaCl demonstrated a reduction in total material loss compared with untreated steel [64]. Tribotesting resulted in the formation of an H_3BO_3 film on the borided surface, contributing to lower wear and friction. Powder-pack

Table 2 Summary of the literature on tribological and tribocorrosion studies of borided steels

Steel material	Case-hardening conditions	Hardness	Wear test method	Observations	Ref.
AISI H13	Powder: 800, 900, and 1000 °C, 2, 4, and 6 h	1930–2600 HV	Ball-on-disc *Counter-body*: WC-Co, RT and 500 °C	Microcrack-induced plastic deformation during the 500 °C wear test. Oxidation and microcrack formation during RT wear tests.	[56]
AISI H13	Powder: 800, 900, and 1000 °C, 6 h	1000–2000 HV	Ball micro-abrasion test *Counter-body*: AISI 52100	Higher boriding temperature increased the thickness of the borided layer, which resulted in a higher wear resistance.	[57]
AISI D2	Powder: 900, 1000 °C, 3, 5, and 7 h	1000–2300 HV	Ball-on-flat, *counter-body*: Al_2O_3	Higher boriding temperature – higher thickness, higher K	[58]
AISI 316L	Powder: 850, 950, and 1050 °C, 2, 4, and 6 h	300–1700 HV	Ball-on-disc *Counter-body*: Al_2O_3	Lower boriding temperatures (850 °C) required longer exposure (6 h) to reduce wear, while higher temperatures (1050 °C) achieved better tribological performance at shorter exposures (2–4 h), as prolonged exposure (6 h) reduced mechanical resistance.	[59]
High-manganese steel	Powder pack: 850, 900, and 950 °C for 2, 4, and 6 h	1100–1800 HV	Ball-on-flat *Counter-body*: WC-Co, RT and 800 °C	The process time and temperature increased the thickness of the borided layer. Lower wear was achieved with higher process temperature. No correlation between the process parameters and friction.	[6]
AISI D2	Powder pack: N/A	1569 HV	Knife mill *Counter-body*: woody biomass	Borided D2 tool steel blades had 3 × higher wear resistance than untreated M2 tool steel blades. Abrasive and erosive wear.	[15]
AISI D2	Powder pack: N/A	1411 HV	Shredder *Counter-body*: corn stover	Borided D2 tool steel cutters had 10 × higher wear resistance than untreated D2 tool steel cutters. Abrasive and erosive wear.	[60]
31CrMoV9 and H13	Paste boriding 900 °C, 4 h 950 °C, 6 h	2000 HV 2185 HV	Ball-on-disc *Counter-body*: Al_2O_3	Wear resistance decreased at 950 °C process temperature due to cracking at the contact region.	[55]
AISI 4130	Powder: 660 °C, 5, 8 h Nitrocarburing + boriding: 660 °C, 5, 8 h	2030 HV 2340 HV	Ball-on-disc *Counter-body*: Al_2O_3	Boriding reduced COF, wear, and corrosion compared to nitrocarburised and duplex treatment of boronitrocarburised steels 5 and 8 h process times produced thicker boride layers and induced formation of superhard phases such as FeB, Fe2B, CrB, MnB, and MnB2, resulting in high hardness and low COF	[5]
AISI 9310	Electrochemical: 510 °C, 1 h, and powder carburized + electrochemical boriding	1500–2000 HV	Ball-on-flat and cylinder-on-flat *Counter-body*: AISI 52100 Oil (PAO)	Borided surface was significantly more wear resistant than the carburized. Boron nitride additives in a gear oil chemically reacted with the borided surface to form a wear protective tribofilm.	[61]
AISI H13	Powder pack: 950 °C, 6 h	22.5 GPa	Ball-on-flat, *Counter-body*: Al_2O_3 Dry and oil (SAE 10W-40)	Smearing and pitting wear. Boriding had no effect on friction.	[62]
AISI 4140	Powder: 900 °C, 1 h + heat treating	B 17.2 GPa B + HT 15.3 GPa	Ball-on-flat, *Counter-body*: engine oil (FE 5W-30)	Wear mechanisms were cracking, grooving, pitting, plastic deformation, and flaking. Boriding and heat treating resulted in better absorption of fluids	[63]
AISI 4140	Powder	19 GPa	Pin-on-disc *Counter-body*: Al_2O_3 *Solution*: 3.5% NaCl	Formation of a boric acid film on borided surfaces, contributing to a lower friction Formation of H_3BO_3 reduced wear in the borided steel, while the unborided specimen experienced increased wear due to iron hydroxide formation.	[64][a]
AISI 316L	Powder: 1000 °C, 4 h	20 GPa	Ball-on-flat *Counter-body*: Al_2O_3 Hanks solution	Powder pack borided AISI 316 tested in Hank's solution had 1.5 times lower wear than the untreated steel [campos-silva]. Untreated steel experiences accelerated wear after the passive film is removed. In the triborrosion testing.	[65][a]

[a]Tribocorrosion studies.

borided AISI 316 tested in Hank's solution had 1.5× less wear than the untreated steel [65]. Untreated steel experienced wear-accelerated corrosion and significant wear after the passive film was removed in the tribocorrosion testing. However, the treated steel was more sensitive to the synergistic effects of wear and corrosion, whereas wear remained the dominant factor in the untreated steel. This increased sensitivity may be due to boride particles detaching, acting as third bodies and further inducing abrasive wear and increasing the corrosion process.

Although the boriding treatment positively influences hardness, wear resistance, and tribocorrosion behavior, the high-temperature process can negatively impact the bulk properties of steel alloys. Boron precipitation in combination with elevated temperatures can lead to phase transformation and grain coarsening [66,67]. High-temperature boriding can also lead to the development of residual stresses in the adjacent substrate area [68].

These review studies demonstrate that the tribological and tribocorrosion performance of steel materials can be significantly

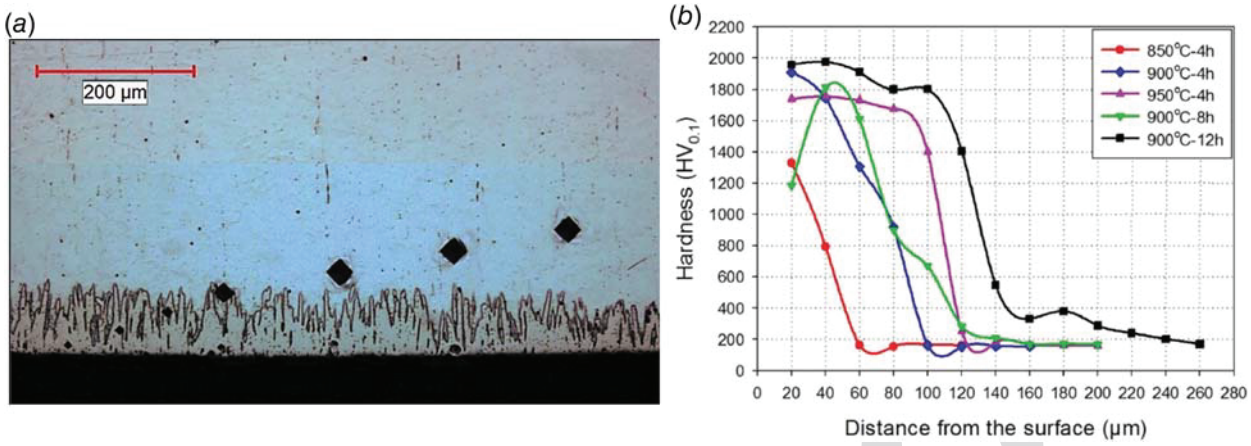

Fig. 5 Influence of process temperature and time on borided SAE 1020 steel (*a*) cross section and (*b*) hardness. Reproduced from Ref. [54] (modified). Copyright 2019 by Elsevier.

enhanced by boriding surface treatment. The wear resistance and hardness seem to increase with the thickness of the borided layer in tool steels. In other types of steel materials, the relationship between the wear resistance, hardness, and thickness of the borided layer varied. The FeB and Fe_2B phases play a role in the hardness as well as the wear and tribocorrosion resistance. Zimmerman [19] pointed out that the formation of a dual FeB and Fe_2B phase is not desirable, and a single Fe_2B phase could provide enhanced wear resistance. The outermost FeB phase is harder and more brittle than the Fe_2B phase. Mismatch in hardness and stress state can lead to the formation of cracks, reduce the integrity of the borided layer, and essentially impair the wear, although the dual phase has not been found to enhance synergistic effects between wear and corrosion during tribocorrosion tests [65]. Subsequent vacuum or salt-bath treatment and conventional heat treatment can mitigate these issues by minimizing the FeB phase in a double-phase boride layer. Oil lubrication improves the wear and friction of the borided steel materials; however, the literature lacks studies on the chemical compatibility of the borided layer with oil lubricants and the mechanics of formation of a protective tribofilm. Further research could expand the application of boriding surface treatment of steel materials in applications with oil-lubricated sliding contact.

3.3 Nitriding. In the nitriding process, nitrogen is diffused into the surface of metals to create a hard, wear-resistant, and corrosion-resistant surface layer [16,21,69]. The advantage of the nitriding process is that it requires low temperatures, up to 600 °C [36], which is much lower than in boronizing, carburizing, or chromizing methods and which eliminates the need for subsequent quenching. The lower process temperature is below the austenitizing temperature, which minimizes grain coarsening of the substrate to preserve the bulk properties. The hardness of the nitride layer can reach up to approximately 1700 HV [1], which is higher than the hardness of the carburized layer but lower than that of the borided and chromized layers. The nitriding surface treatment is typically used for high-alloy ferrous materials. Alloying elements such as molybdenum, aluminum, vanadium, or chromium are needed to promote nitriding by forming nitrides to enable high hardness and wear resistance; therefore, low-alloy steels are less suitable for nitriding [16]. The nitriding process forms a diffusion zone composed of nitrides along with a thinner compound layer containing ε and γ' iron nitride phases [16,36,66], as shown in Fig. 6 [66]. This zone can be up to 25 μm thick [36]. Nitriding surface treatment can be accomplished by gas, plasma, or salt-bath-nitriding processes. Among those, gas nitriding is the preferred process because of its precision, throughput, and relatively low cost.

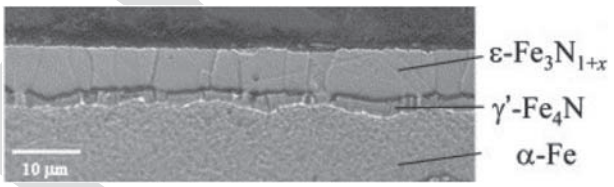

Fig. 6 A compound nitrided layer composed of ε and γ' formed by nitriding at 550 °C for 5 h on an iron specimen. Reproduced from Ref. [66] (modified). Copyright 2003 by Elsevier.

The reviewed studies, summarized in Table 3, explored the effect of nitriding temperature, time, and sources on the tribological performance of stainless steels, tool steels, and low-alloy steel prepared by plasma nitriding. Several studies showed that increasing nitriding time increases the depth of the nitriding layer, thereby increasing the hardness. AISI 4140 steel treated with plasma and pulse-plasma nitriding with 17 and 28 h process times developed a deeper nitride layer with the longer (28 h) duration in both methods [67]. The depth of the layer and nitrogen concentration positively affected the hardness; however, the higher hardness negatively affected the wear resistance. At higher contact loads, the hard and thick nitrided layer experienced a brittle failure, which generated hard abrasive particles during sliding and led to decreased wear resistance. A similar observation was made during plasma-nitriding of AISI H13 tool steel, where a thicker nitride layer formed because of a longer nitriding time, exhibiting lower wear resistance and higher hardness than a thinner layer achieved with shorter process time [72]. However, contradicting trends were observed in ion and plasma nitriding of AISI H13 steel at varying process times [73]. The study revealed an increase in hardness and a decrease in wear rate and friction with increasing nitriding time, as shown in Fig. 7 [73]. The improvement in the hardness and tribological behavior was attributed to the formation of hard Fe_4N, Fe_3N, and CrN phases for a 12-h process time, whereas 3- and 6-h process times produce only the α-Fe phase. The study also showed that the ion plasma-nitriding process had more positive effects on the tribological performance compared with the neutral plasma nitriding, owing to reduced surface roughness.

The role of nitriding temperature on tribological performance was also investigated in several studies. Plasma-nitriding treatment of AISI H11 and AISI M7 tool steels conducted at 450 and 520 °C showed that wear rate and friction both decreased with a higher process temperature [75]. By contrast, a study on plasma nitriding of M50 tool steel found inconsistent trends between the nitriding temperature, which ranges from 450 to 540 °C, and the tribological performance [70]. The optimal combination of hardness, wear

Table 3 Summary of the literature on tribological and tribocorrosion studies of nitrided steels

Steel material	Case-hardening conditions	Hardness	Wear test method	Observations	Ref.
M50	Plasma: 480–540 °C, 8 h	1200 HV	Pin-on-disc *Counter-body*: WC-Co	500 °C process temp. results in optimum hardness and wear Temperature affected the formation of surface nitrides and carbide precipitation.	[70]
AISI 316L	Plasma: 550 °C, 1 h	960 HV	Ball-on-disc *Counter-body*: AISI 52100	Adhesive and oxidation wear	[71]
AISI 4140	Plasma: 540 °C, 17 and 28 h	940 HV	Pin-on-disc AISI 52100	Higher nitrogen content produced a thicker case layer	[67]
AISI 4140	Plasma and pulse plasma: 540 °C, 17 and 28 h	970 HV	Pin-on-disc *Counter-body*: AISI O2	Pulsed plasma treatment produced a thicker case layer and higher hardness due to higher nitrogen content. Longer process times resulted in lower wear resistance due to a very hard layer.	[67]
AISI H13	Plasma: 530 and 550 °C, 4, 16, 49, and 100 h	1300 HV	Disc-on-flat *Counter-body*: N/A	Thicker nitride layer with longer process times. Higher wear rate with thicker layers due to spalling. Adhesive and abrasive wear.	[72]
AISI H13	Plasma: 500 °C, 1.5–6 h Neutral nitriding: 500 °C, 3–12 h	1400 HV 1400 HV	Ball-on-disc *Counter-body*: SUJ2	Layer thickness increased with process time. Wear rate decreased with process time. A lower wear rate was achieved with the plasma method.	[73]
AISI 304L	Plasma: 375–475 °C, 0.6–16 h	3–20 GPa	Pin-on-disc *Counter-body*: ruby, 100Cr6, PTFE, aluminum, stainless steel	Hardness increases with process time, temperature, higher pulse duration/pulse pause ratio.	[74]
AISI H11 and AISI M7	Plasma nitriding: 450–520 °C, 2 h	N/A	Rolling and pin-on-disc *Counter-body*: AISI 52100	Lower wear and friction versus untreated steel.	[75]
Nitralloy 135M	Gas: 985 °C, 6 h	1300 HV	Cone-three-cylinder test *Counter-body*: N/A	The wear is linear at medium loads but increases rapidly at higher loads.	[21]
304	Salt bath	5150 N/mm^2	Ball-on-disc *Counter-body*: ZrO_2 base oil	Higher wear resistance due to the lower surface energy of the nitrided surface layer.	[76]
UNS S32750 super duplex stainless steel	Plasma: 300, 350, and 400 °C, 4 h	13 GPa	Ball-on-flat *Counter-body*: Si_3N_4 *Solution*: 0.5 M NaCl	Process temperature increased N content, which resulted in the improvement of the tribocorrosion resistance.	[77][a]
AISI 316L and 2205 duplex stainless steel	Plasma: 450 °C, 10 h	1300 HV 1500 HV	Ball-on-flat *Counter-body*: Al_2O_3 *Solution*: 3.5% NaCl	Thicker, harder S-phase in duplex stainless steel improves depassivation resistance and reduces material loss but may accelerate loss under high loads due to galvanic coupling.	[78][a]
316L	Plasma: 415 °C, 15 h	1200 HV	Ball-on-flat *Counter-body*: Al_2O_3 *Solution*: 0.5 M H_2SO_4	Poor tribocorrosion performance due to metal dissolution in the H_2SO_4 environment.	[45][a]
AISI 1020 mild steel	Plasma: 550 °C, 5 h	760 HV	Ball-on-flat *Counter-b`ody*: Al_2O_3 1.0 wt% NaCl	Formation of a ε-Fe_4N ~87% wear reduction under anodic conditions	[79][a]
AISI P20 plastic mould steel	Nitrocarburized, gas-nitrided, and salt bed nitrided: 560 °C, 8 h Plasma: 520 °C, 8 h	895 HV	Ball-on-flat *Counter-body*: Al_2O_3 *Solution*: 3.5 wt% NaCl	Plasma-nitrided and -nitrocarburized samples had a lower corrosion tendency under sliding conditions due to denser layers.	[80][a]

[a]Tribocorrosion studies.

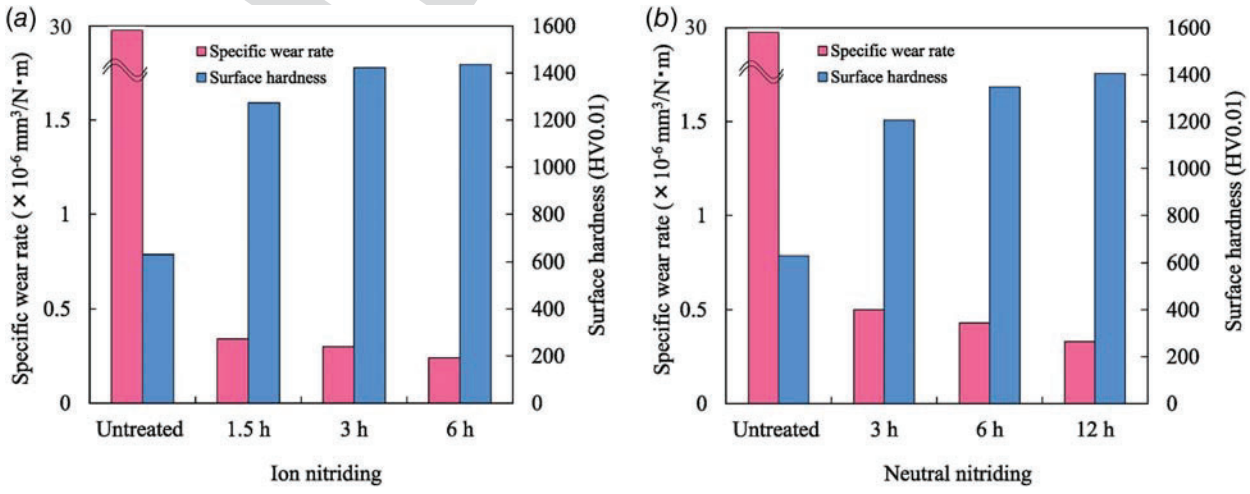

Fig. 7 Wear rate and hardness of AISI H13 tool steel nitrided at 500 °C as a function of process time using (*a*) ion (plasma) and (*b*) neutral (gas) nitriding methods. Reproduced from Ref. [73]. Copyright 2019 by Elsevier.

resistance, and friction performance was achieved with a 500 °C nitriding temperature in which stable MC and M_6C precipitates were formed.

Effects of plasma nitriding on the subsequent physical vapor deposition nitride coatings were also explored. Podgornik et al. [67] investigated the tribological performance of AISI 4140 pretreated with plasma nitriding and coated with TiN, TiAlN, and ta-C. The study showed that nitriding improved the adhesion of the physical vapor deposition coating to the substrate, leading to improved tribological performance. Similar positive effects of plasma nitriding have been shown in AISI 316L steel coated with CrWAlTiN [71]. The duplex treatment resulted in higher wear resistance and hardness than the coated steel without nitriding. The main wear mechanism of the duplex-treated AISI 316L was oxidative.

Methods other than plasma nitriding were also reviewed. A study on the salt-bath nitriding of 304 steel demonstrated that the improvement in the wear and friction performance compared with the untreated base in oil-lubricated conditions is due to smaller surface energy and larger contact angle of the nitride layer, which inhibits the removal of abrasive particles from the sliding surface [76]. Gas nitriding of nitralloy 135M steel showed that the wear is linear at a mild load, but when the contact pressure exceeds 200 MPa, the wear increases rapidly [21].

Most of the studies on tribocorrosion characterization focused on stainless steels. Haruman et al. [78] reported enhanced tribocorrosion resistance of 316L stainless steel and duplex stainless steel in NaCl solution compared with untreated 316L stainless steel and untreated duplex stainless steel, respectively. The thicker and harder S-phase layer on the treated duplex stainless steel exhibited superior resistance to depassivation and lower material loss than treated 316L stainless steel. Notably, when the substrate was exposed to a higher applied load, the treated layer established a galvanic coupling with the substrate and experienced rapid material loss, as observed in 316L stainless steel. Sun and Bailey [45] conducted a comparative study on the tribocorrosion behavior of low-temperature nitrided and carburized 316L stainless steel in 0.5 M H_2SO_4 solution. In dry sliding wear tests, the nitride layer provided superior wear resistance owing to its higher hardness, but in tribocorrosion tests under open circuit potential conditions, the carburized layer improved 316L stainless steel resistance by 40%, while the nitrided layer performed worse than untreated steel. The poor tribocorrosion of the nitrided 316L stainless steel was due to metal dissolution. The study concluded that low-temperature nitriding is not suitable for H_2SO_4 environments. Possoli et al. [77] investigated tribocorrosion performance, particularly the repassivation behavior, of low-temperature plasma-nitrided super duplex stainless steel in 0.5 M NaCl solution and pointed out that higher nitrogen content can enhance both the repassivation ability and the load-bearing capacity, leading to higher tribocorrosion resistance.

Tribocorrosion of other steel types was also investigated. A study on tribocorrosion of a plasma-nitrided AISI 1020 mild steel in NaCl solution showed that a nitrided layer containing ε-Fe_4N enhances the tribocorrosion resistance owing to its high wear resistance and ability to reduce metal dissolution, thereby reducing total material removal by about 87% under anodic conditions [79]. The study emphasized that effective resistance to tribocorrosion depends on preventing localized surface damage because sliding in NaCl solution can lead to accelerated pitting corrosion and increased material loss. Boztepe et al. [80] investigated the influence of different nitrided and nitrocarburized treatments on the corrosion and tribocorrosion of AISI P20 plastic mold steel. Testing with a 3.5 wt% NaCl solution showed that plasma-nitrided samples treated at 520 °C for 8 h and nitrocarburized samples treated at 560 °C h exhibited lower tribocorrosion than gas-nitrided and fluidized bed-nitrided samples because they had a denser and more compact layer.

The passivation mechanisms of the nitride layer of AISI 316L and 304L stainless steels were investigated in Ref. [81]. High nitrogen concentrations in the nitride layer were found to negatively affect the corrosion resistance due to the formation of chromium nitride (CrN) precipitates. In contrast, lower nitrogen concentrations improved the passivation behavior. This was attributed to an initial increase in anodic dissolution, which accelerated the formation of corrosion products that subsequently precipitated and contributed to the development of a passive film. Additionally, the accumulation of nitrides, such as CrN, on the corroded surface was found to further enhance passivation.

The reviewed studies suggest that the tribological performance of the nitrided ferrous alloys is strongly influenced by the thickness and hardness of the nitrided layer. Although higher hardness and thickness of the layer may seem to improve the wear resistance, an overly thick and hard nitrided layer could be a disadvantage. Higher contact loads could lead to brittle failure and spalling of the nitride layer, thereby reducing the wear resistance. This effect could be more notable in erosive wear, in which fracture toughness plays an important role. Karamis suggested that a thinner and more ductile layer composed of γ'-Fe_4N phase can be more beneficial than a thicker ε-$Fe_{2-3}N$ or γ'-Fe_4N compound in achieving optimal wear resistance [72,82]. The tribological characterization of nitrided ferrous alloys also showed that the wear mechanisms are mainly abrasive, oxidative, and adhesive. The thickness and hardness of the nitride layer also affect tribocorrosion resistance, particularly when mechanical wear is the dominant factor in material loss. Similar to carburizing, nitriding was also reported in some case studies to improve the tribocorrosion resistance of steels. As observed in stainless steel system [81], high nitrogen concentrations may negatively affect corrosion resistance due to the formation of precipitates. In contrast, lower nitrogen levels enhance passivation by promoting anodic dissolution, facilitating the formation of corrosion products, and enhancing the accumulation of nitrides that contribute to passive film development.

3.4 Nitrocarburizing. In the nitrocarburizing process, carbon and nitrogen are simultaneously diffused into the surface of metals to enhance their hardness as well as wear and corrosion resistance [21,83]. This technique can be applied to a wide range of ferrous materials, including low-carbon steels, low-alloy steels, tool steels, stainless steels, and cast iron. Similarly to the nitriding process, nitrocarburizing does not require subsequent quenching because of its lower process temperatures up to 600 °C [83]. Lower process temperatures have less impact on the bulk microstructure and consequently preserve the bulk properties. The nitrocarburizing process results in the formation of a diffusion zone, which consists of nitrides and carbonitrides, and a compound layer, which consists of ε-Fe_2N_{1-z} and γ'-Fe_4N_{1-x} iron nitride phases and is affected by the process parameters, as shown in Fig. 8 [84]. The nitrocarburized compound layer can be up to 25 μm thick [36] with a hardness of 700–1200 HV based on the studies reviewed herein. Nitrocarburizing is typically carried out in gas, salt bath, and plasma media.

The reviewed literature on nitrocarburized ferrous alloys, summarized in Table 4, covers plasma, gas, and salt-bath processes as well as different process temperatures and durations for tool steels, low-alloy steels, stainless steels, and cast iron. The effect of process temperature on the composition of the nitrocarburized layer and its tribological behavior was demonstrated via plasma nitrocarburization of AISI 4140 at 530, 570, and 630 °C [89]. The highest hardness and wear resistance and the lowest friction were achieved with 570 °C process temperature, as shown in Fig. 9 [89]. Further analysis showed that ε and γ' phases were present in the compound layer at all process temperatures. Although the thickest layer was produced at 630 °C, the highest amount of the harder ε phases was found in the layer produced at 570 °C. The higher concentration of the harder phase was likely responsible for the improved hardness and the tribological performance. The effect of process temperature was also investigated in plasma nitrocarburization of M50NiL steel [85]. The amount of ε-Fe_{2-3}(N,C) and γ'-Fe_4N(N,C) phases increased with process temperature (460, 500, and 540 °C), thereby increasing the hardness of the

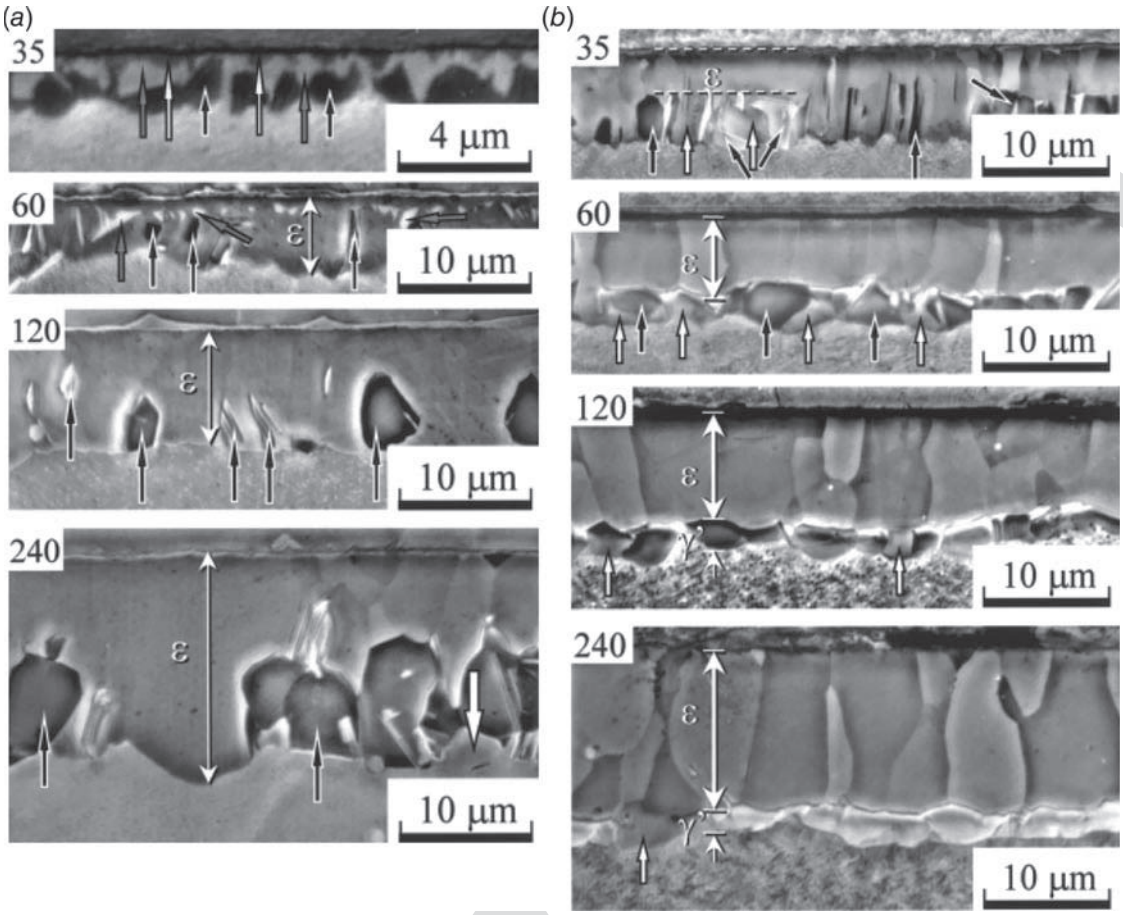

Fig. 8 Micrographs of gas-nitrocarburized iron cross sections with process times (minutes) indicated in the upper left corners and varying gas mixtures. (*a*) 10.08 m^3/h gas flow and 11.09% vol. content of HN_3 and (*b*) 21.4 m^3/h gas flow and 35.14% vol. content of NH_3. Black arrows: γ'-Fe_4N_{1-x} phase; white arrows: ε-Fe_2N_{1-z} phase; gray arrows: cementite phase. Reproduced from Ref. [84]. Copyright 1969 by Springer Nature.

Table 4 Summary of the literature on tribological and tribocorrosion studies of nitrocarburized steels

Steel material	Case-hardening conditions	Hardness	Wear test method	Observations	Ref.
M50NiL	Plasma: 460–540 °C, 4 h	1287 HV	Pin-on-disc *Counter-body*	Hardness increased with temperature. Oxidative and abrasive wear. Optimal wear performance at 500 °C.	[85]
DC53	Salt bath: 570 °C, 2, 4, and 6 h	1120 HV	Slurry-erosion test *Counter-body*: SiC particles	Erosion rate decreases with higher process time. Max. erosion at 30 deg angle.	[86]
AISI H13 and Cr–Mo–V	Salt baths: 580 °C, 4 h	1000 HV	Ball-on-disc *Counter-body*: Al_2O_3	AISI H13 had a deeper case than Cr–Mo–V Treatment had no effect on friction but reduced micro-ploughing and oxidation	[87]
316	Salt bath: 570–610 °C, 15:135 min Cyanate: 25–45%	246 HV	Pin-on-disc *Counter-body*: N/A	Higher process time and temperature resulted in increased thickness and hardness, and reduced wear. Cyanide concentration and temperature are the most significant parameters.	[88]
AISI 4140	Plasma: 530, 570, and 630 °C, 5 h Voltage: 720, 800, and 850 V	800 HV	Pin-on-disc *Counter-body*: AISI 52100	570 °C process temperature resulted in the highest hardness, wear resistance, and lowest friction due to the highest amount of harder ε-Fe_{2-3} phases.	[89]
AISI 431	Plasma (electrolytic): 5–15 min Voltage: 150–180 V	19 GPa	Pin-on-disc *Counter-body*: Si_3N_4	Wear and friction decrease with increasing process time due to a denser layer. Adhesive wear and spalling.	[90]
AISI H11	Gas: 525 °C, 5.5 h	1050 HV	Pin-on-disc *Counter-body*: WC-Co	Abrasive and oxidative wear. Oxide tribo-film formed on the nitrocarburized surface.	[91]
HT250 gray cast iron	Gas: 560 °C, 1.6 h	460 HV	Ball-on-disc *Counter-body*: AISI 52100	Spalling wear and three-body abrasive wear.	[92]
AISI P20 plastic mould steel	Nitrocarburized, gas-nitrided, and salt bed nitrided: 560 °C, 8 h Plasma: 520 °C, 8 h	888 HV	Ball-on-flat *Counter-body*: Al_2O_3 *Solution*: 3.5 wt% NaCl	Plasma-nitrided and -nitrocarburized samples had a lower corrosion tendency under sliding conditions due to denser layers.	[80][a]

[a]Tribocorrosion studies.

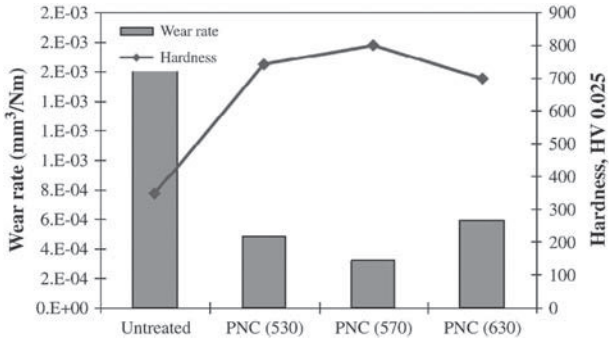

Fig. 9 Wear rate and hardness of plasma-nitrocarburized AISI 4140 steel for different process temperatures: 530, 570, and 630 °C. Reproduced from Ref. [89]. Copyright 2010 by Elsevier.

nitrocarburized layer. The primary wear mode transitioned from oxidative to abrasive with increasing sliding speeds.

The effect of nitrocarburizing duration has also been investigated. Slurry-erosion testing on DC53 tool steel nitrocarburized for 2, 4, and 6 h showed that longer process times decreased the erosion rate [86]. Longer process time also led to greater diffusion depth of the nitrocarburized layer, which was associated with improved abrasion resistance. The nitrocarburizing treatment also altered the wear mode, changing it from adhesive to abrasive.

To better understand the combined effects of nitrocarburizing process time, temperature, and solution on tribological behavior, Jeyakymar et al. [88] applied Taguchi optimization experimental design. In this study, 316 stainless steel was nitrocarburized using the salt-bath method at temperatures of 570–610 °C, process times of 115–135 min, and cyanate concentrations of 25–45%. The study revealed that the diffusion depth and hardness are positively influenced by higher process temperatures and times. The highest hardness and the highest wear resistance were achieved with 35% of cyanide, 590 °C temperature, and 135-min process time. The study also concluded that cyanide solution and temperature are the parameters that have the most significant effect on wear performance.

The influence of base material composition on the nitrocarburizing process was studied on salt-bath-nitrocarburized AISI H13 hot-work tool steel and Cr–Mo–V cold-work steel [87]. The hot-work steel had a deeper nitrocarburized layer than the cold-work steel because of its higher concentration of vanadium. By contrast, higher chromium content in Cr–Mo–V cold-work steel inhibited the diffusion process. However, the nitrocarburizing process seemed to be more beneficial for Cr–Mo–V cold-work steel because the wear was reduced by 85%. The wear reduction in AISI H13 steel was 55% compared with the untreated base. Although the nitrocarburizing process reduced the micro-ploughing and oxidative wear in both steel materials, friction performance was not noticeably affected.

Other reviewed studies focused on characterizing the wear mechanism of nitrocarburized steels. Tribological characterization of gas-nitrocarburized AISI H11 tool steel showed that the primary wear modes are mild two-body abrasion and oxidative wear [91]. The study also reported the formation of tribofilm composed of chromium- and vanadium-alloyed iron oxides. Tribological testing of gas-nitrocarburized gray cast iron showed surface spalling and three-body abrasive wear [92].

The reviewed literature on tribological characterization of nitrocarburized ferrous alloys shows that surface treatment improves hardness and wear resistance. Similar to other case-hardening methods, the thickness of the nitrocarburized layer tends to increase with increasing process time and temperature, thereby increasing hardness. However, the tribological performance depends on the combination of the process parameters, including the compound composition, which needs to be optimized. Composition of the base material can affect the diffusion process: vanadium promotes diffusion, whereas chromium tends to inhibit it. The composition of the compound layer also affects the tribological behavior, and a higher concentration of ε-$Fe_{2-3}N$ phase can improve wear resistance. The primary wear modes were identified as abrasive and oxidative. Only a few studies investigated tribocorrosion of nitrocarburized steels. Tribocorrosion of gas-nitrocarburized AISI P20 plastic mold steel is discussed in Sec. 3.3 [80]. According to the limited literature on tribocorrosion studies of nitrocarburized steels, nitrocarburizing may have the potential to enhance tribocorrosion resistance because of its lower corrosion tendency and the structure of the compound layer [80].

3.5 Carbonitriding. Carbonitriding is a similar process to nitrocarburizing: it diffuses carbon and nitrogen to enhance hardness as well as wear and corrosion resistance. However, carbonitriding uses a higher concentration of carbon [18]. Similar to the carburizing process, carbonitriding is typically applied to low-carbon and low-alloy ferrous metals to increase their hardness as well as wear and corrosion resistance [18]. Adding nitrogen benefits the material by improving hardness, wear resistance, and process times compared with the carburizing process. Carbonitriding is carried out in three media: gas, salt bath, and plasma [18]. The process temperatures are typically up to 900 °C [1], which is similar to carburizing temperatures but higher than nitriding and nitrocarburizing temperatures. During the process, carbon diffuses deeper into the surface because it has higher diffusivity than nitrogen and forms a carbon-rich case with martensite structure upon quenching, as shown in Fig. 10 [93]. In some cases, a very thin compound layer consisting of carbide and nitride phases can form [90,94]. Carbonitrided diffused layers can be up to 750 μm deep [95] and reach hardness up to 850 HV [36]. These values are higher than those from carburizing but lower than those from boriding and chromizing processes.

The reviewed studies shown in Table 5 covered tribological characterization of carbonitrided stainless steels and high-carbon low-alloy steels prepared by gas and plasma techniques. The influence of nitrogen concentration on the tribological behavior in the carbonitrided process was demonstrated on AISI 52100 steel [94]. Varying the addition rate of NH_3 gas in a range of

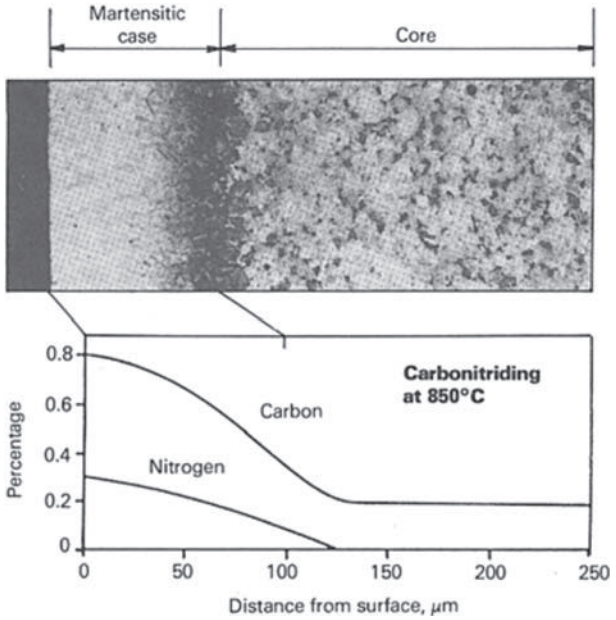

Fig. 10 Optical image of cross-sectioned steel carbonitrided at 850 °C. Martensitic case is formed on the outermost surface by introducing high concentrations of carbon and nitrogen. Reproduced with permission from Fastener Technology International magazine, www.fastenertech.com [93].

Table 5 Summary of the literature on tribological studies of carbonitrided steels

Steel material	Case-hardening conditions	Hardness	Wear test method	Observations	Ref.
AISI 1020 and 5115	Gas: 860 °C, 3.5 h compared to carburizing and boriding	1020: 750 HV 5115: 830 HV	Ball-on-disc *Counter-body*: borided AISI 8640	Carbonitriding had a better effect on low-carbon–low-alloy 1020 steel than on alloy 5115 steel. Carbonitriding resulted in lower wear and friction than carburizing but did not outperform boriding treatment.	[25]
316LVM medical-grade stainless steel	Plasma: 430 °C, 15 h	13.3 GPa	Ball-on-flat fretting test *Counter-body*: AISI 440C	Carbonitriding reduced adhesive wear due to higher hardness compared to the untreated. Mild abrasion.	[96]
AISI 52100	Gas: 835 °C, 210 min NH_3 addition rate: 0.28–1.2 l/min	748 HV	Pin-on-disc *Counter-body*: AISI 52100	Highest level of nitrides 0.4-l/min NH_3 rate, which resulted in the highest wear resistance and hardness.	[94]
C45	Laser	822 HV	Ball-on-disc *Counter-body*: Si_4N_4	Abrasive and adhesive wear.	[97]
AISI 321 stainless steel	Plasma: 350–650 W	N/A	Ball-on-disc *Counter-body*: WC-Co	Higher laser power increased layer thickness and reduced wear.	[98]
AISI 1045	Plasma Voltage: 260:300 V Time: 2:10 min Carbamide: 10:20 wt%	890 HV	Ball-on-disc *Counter-body*: Si_3N_4	Higher voltage, time, and carbamide concentration increased hardness Mixed wear-rate trends.	[99]
AISI 431	Plasma (electrolytic): 5–15 min Voltage: 150–180 V	19 GPa	Pin-on-disc *Counter-body*: Si_3N_4	Wear and friction decrease with increasing process time due to increased thickness and density of the layer. Adhesive wear and spalling.	[90]
M50NiL	Carburizing, sequential carburizing, and nitriding	1200 HV	Ball-on-disc *Counter-body*: WC-Co	Nitriding after carburizing was shown to increase the hardness and wear resistance and reduce friction compared with the carburizing treatment.	[100]

0.28–1.20 L/min revealed that the volume fraction of retained austinites increases with increasing NH_3 rate, and the highest levels of $(Cr,Fe)_2N_{1-x}$ nitrides were found at an NH_3 addition rate of 0.40 L/min. Because the best wear performance and hardness were achieved at this rate, the nitride concentration was shown to be the key factor. The carbonitriding process reduced the adhesive and oxidative wear, which were the dominant modes in the untreated AISI 52100 steel.

A study on plasma carbonitriding of AISI 321 steel investigated the effects of process temperature on its tribological behavior [98]. Carbonitriding by varying the plasma power at temperatures from 390 to 690 °C showed that higher process temperatures enabled by higher plasma power yield a thick, hard, carbonitrided layer, essentially leading to better tribological performance. An amorphous carbon–nitrogen compound layer formed at process temperatures above 450 °C, improving the wear resistance. The lowest wear and friction were achieved at the highest temperature of 690 °C.

Chongyang et al. [99] investigated the effect of plasma voltage, treatment time, and concentration of carbamide and NH_4Cl on the tribological behavior of plasma-carbonitrided AISI 1045 steel. The study showed that the thickness of the case layer is significantly influenced by the plasma voltage and process time. The higher plasma voltage (5 and 10 V) and longer treatment time (5 and 10 min) resulted in a thicker layer; however, the extremely thick layer was shown to affect its quality. The highest hardness was achieved with 20% carbamide, 5% NH_4Cl, 280 V, and 10 min process time, whereas the 2-min (shortest) process time resulted in the lowest wear. A positive influence of voltage and time on the hardness was also demonstrated in plasma electrolytic carbonitriding of AISI 431 steel [90]. Increasing voltage from 150 to 180 V and time from 5 to 15 min were shown to increase thickness and improve the density of the diffused layer, resulting in higher hardness. Increasing process time resulted in lower wear and friction, as shown in Fig. 11 [90]. Although carbonitriding reduced oxidative wear, adhesive wear with spalling of the layer was observed.

Selçuk et al. [25] compared the tribological performance of carbonitrided AISI 1020 and 5115 steels with those of their carburized and borided counterparts. The study concluded that the carbonitriding treatment is more beneficial to these low-carbon, low-alloy steels than the carburizing treatment. However, the borided treatment resulted in the overall lowest wear and friction. Wear and friction were lower with carbonitriding treatment than with carburizing but higher than with boriding treatment.

Other studies have simply focused on comparing the tribological performance of carbonitrided steels with that of the untreated steels and characterizing the wear mechanism. Tribological characterization of plasma-carbonitrided 316 LVM medical-grade steel was analyzed with a fretting test [96]. The primary wear mode of carbonitrided 316 LVM was identified as mild abrasion, and the treatment also helped to reduce adhesive wear compared with its untreated counterpart. In laser-carbonitrided C45 steel, the primary wear modes were abrasive and adhesive [97]. Zeng et al. [100] investigated sequential carburizing and nitriding treatment on the tribological behavior of M50NiL steel. Nitriding after carburizing was shown to increase the hardness and wear resistance and reduce friction compared with the carburizing treatment. The improvement in the wear resistance was attributed to the higher hardness. During sliding, the carbonitride particles shrink, which prevents spalling of the case layer.

These reviewed studies suggest that the hardness and tribological performance of carbonitrided ferrous alloys can be improved by higher process temperature and longer process time. Optimal tribological behavior can be achieved by controlling the quality of the case layer by tuning the process parameters. Although only a few studies investigated the influence of a thin compound layer, its presence and thickness improve wear resistance. Abrasive wear seems to be the dominant wear mode of carbonitrided ferrous alloys. The literature does not provide any relevant study on tribocorrosion of carbonitrided steel.

3.6 Chromizing. Chromizing is typically applied to ferrous alloys to enhance their resistance to corrosion and high-temperature oxidation and to improve the hardness, wear, and adhesion resistance [23,24]. The main advantage of chromizing over other case-hardening methods is the enhancement of high-temperature performance and corrosion resistance [23]. Chromizing can be applied to a wide range of ferrous materials; however, the process is more beneficial for low-carbon and low-alloy steels. Chromizing is carried

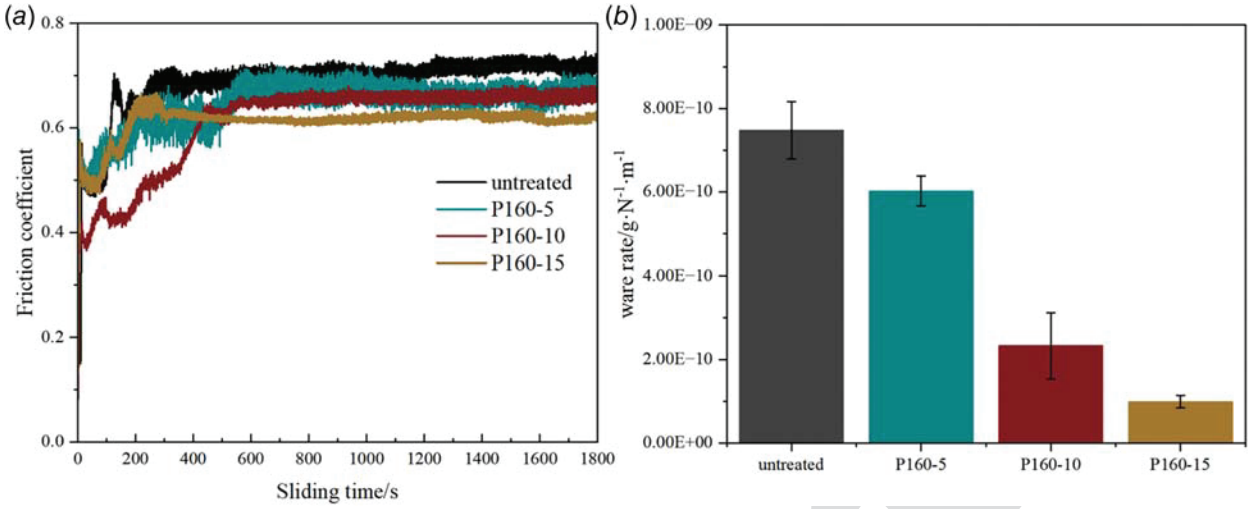

Fig. 11 (*a*) Friction coefficient and (*b*) wear rate of plasma electrolytic carbonitrided AISI 431 for 5, 10, and 15 min at 160 V. Reproduced from Ref. [90]. Copyright 2025 by Elsevier.

out at temperatures of 800–1300 °C [23]. The hardness of the chromized layer can reach up to 1900 HV [27]. The chromized layer typically consists of mixed $M_{23}C_6$, M_7C_3, and M_3C phases [101–103], and its thickness can be affected by the composition of the substrate [23], as shown in Fig. 12 [27]. Chromizing steel materials can be accomplished by powder-pack cementation [27,101,104], gas chromizing [105], molten salt chromizing, or plasma chromizing diffusion techniques. Among these, gas chromizing produces the most uniform layer, and powder-pack cementation is the most affordable [23]. The downside of chromizing is that these process methods are costlier than other case-hardening methods.

Literature on tribological and tribocorrosion characterization of chromized steel materials is summarized in Table 6. Most research has focused on the tribological behavior of chromized steels prepared by conventional powder-pack cementation technique. In a study investigating the effect of chromizing on the abrasive wear of different steel materials, pack chromizing was applied to AISI 1095, AISI 52100, and A2, D2, and M2 tool steels [27], Fig. 12 [27], and Fig. 13 [27]. The study found that chromizing significantly increased hardness in all steel materials, but only AISI 1095, 52100, and A2 steels showed notable wear resistance improvements compared with untreated samples. The differences in the wear performance were attributed to the steel composition: the higher alloy content in D2 and M2 steels decreased chromium diffusion and led to thinner, more porous chromized layers. The effects of steel carbon content and process time were studied in pack-chromized AISI 1020, AISI 1045, and AISI 1095 steels using a scratch test [101]. The thickness of the chromized layer was highest for AISI 1095 and lowest for AISI 1020 steel, suggesting that the chromizing process is favorable for steel with high-carbon content. In all three steel materials, the thickness of the chromized layer increased with increasing cementation time. Critical load measured by scratch test revealed that the scratch resistance for ASI 1045 and 1095 steels improves with increasing layer thickness, and the opposite trends were observed in AISI 1020 steel. The reduced scratch resistance of the thicker chromized layers in AISI 1020 steel was attributed to a thinner $(Cr,Fe)_2N_{1-x}$ phase and decreased adhesion of the $(Cr,Fe)_2N_{1-x}$ and $(Cr,Fe)_{23}C_6$ phases within the chromized layer.

Another study investigated the scratch resistance of chromized AISI 1095 steel prepared by pack cementation as a function of process time (1, 4, and 9 h) and temperature (850 and 900 °C) [104]. The thickness of the chromized layer increased linearly with chromization time for both temperatures, and the thickest layer was achieved with 9 h at 900 °C. The scratch resistance was

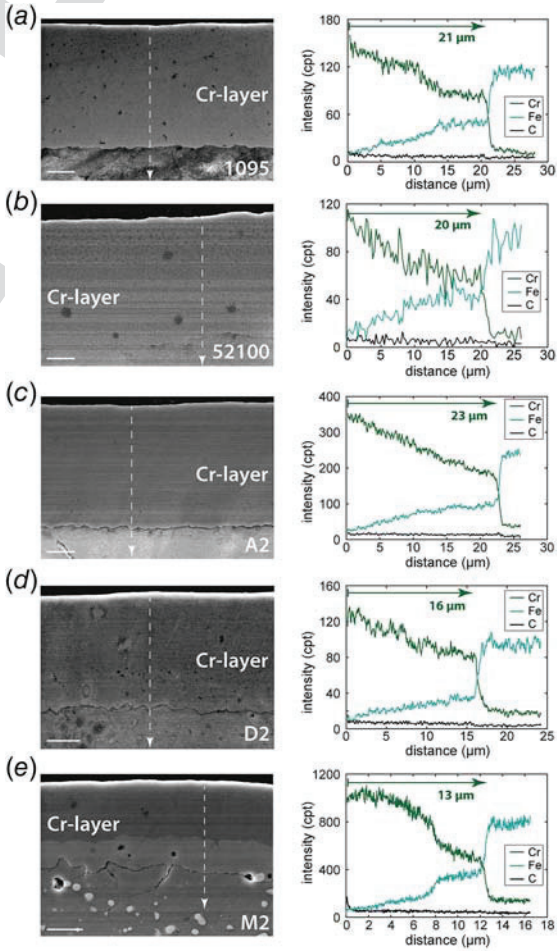

Fig. 12 Thickness and composition of cross-sectioned chromized layers of various steel materials prepared by pack cementation at 980 °C for 8 h analyzed with scanning electron microscopy and energy dispersive spectroscopy elemental line scans. (*a*) AISI 1095, (*b*) AISI 52100, (*c*) AISI A2, (*d*) AISI D2, and (*e*) AISI M2 steel materials. The size of the scale bar is 5 μm. Reproduced from Ref. [27] (modified). Copyright 2023 by Sage Publications.

Table 6 Summary of the literature on tribological and tribocorrosion studies of chromized steels

Steel material	Case-hardening conditions	Hardness	Wear test method	Observations	Ref.
AISI 1095 AISI 52100 A2 D2 M2	Powder: 980 °C, 8 h	1880 HV 1851 HV 1670 HV 1724 HV 1546 HV	ASTM G174 loop abrasion test *Counter-body*: abrasive tape	Chromized 1095, 52100, and A2 had a thicker layer due to their lower alloy content, resulting in the highest enhancement of hardness and wear resistance.	[27]
AISI 1020 AISI 1045 AISI 1095	Powder: 900 °C, 1, 4, and 9 h	19 GPa	Scratch test	Thickness and scratch resistance increase with carbon content and process time.	[101]
AISI 1095	Powder: 850 and 900 °C, 1, 4, and 9 h	N/A	Scratch test	Thickness and scratch resistance increase with process time and temperature.	[104]
T10	Powder: 1000 °C, 24 h	590 HB	Pin-on-disc *Counter-body*: chromized 20CrMnTi	Chromizing reduced the friction and wear of the T10 and 20CrMnTi counter-body.	[106]
52100	Gas: 880 °C	17 GPa[a]	Ball-on-flat *Counter-body*: 52100	Higher contact pressures enabled the formation of a chromium oxide layer, which reduced the wear and friction.	[105]
QT400	Powder: 1000 °C, 1 h	~19 GPa[a]	Ball-on-disc *Counter-body*: 316 stainless steel Dry and oil	Chromizing reduced the wear. Small difference between dry and oil-lubricated conditions.	[107]
C45	Powder chromosiliconized: 1000 °C, 6 h	1430 HV	Cone-three-cylinder test *Solution*: sugar slurry	Chromosiliconizing increased roughness and hardness, with heat-treated layers enhancing wear resistance. Higher loads caused frictional seizure.	[108][a]
C45	Powder: 1050–1150 °C		Disk-on-plate *Solution*: salt water	Chromized improved tribocorrosion resistance in salt water compared to the untreated one	[109][a]

[a]Tribocorrosion studies.

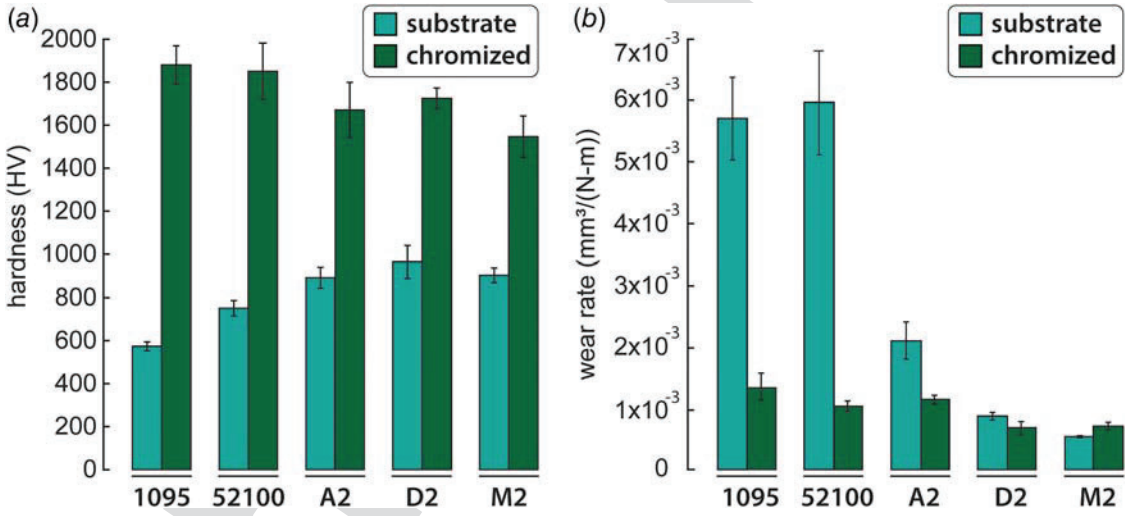

Fig. 13 Hardness and abrasive wear resistance of chromized and untreated: AISI 1095, AISI 52100, AISI A2, AISI D2, and AISI M2 steel materials. Chromizing was carried out at 980 °C for 8 h. Reproduced from Ref. [27]. Copyright 2023 by Sage Publications.

positively correlated with the thickness of the chromized layer. Similar to the findings from the previous study [101], the improved scratch resistance was attributed to the thicker $(Cr,Fe)_2N_{1-x}$ phase and higher adhesion of the phases within the chromized layer.

A study comparing the tribological behavior of chromized and untreated T10 and 20CrMnTi steel friction pairs tested by pin-on-disc sliding contact showed that chromizing increases wear resistance and reduces friction [106].

The tribological behavior of chromized steel materials made by the gas-chromizing technique was also investigated. A study on the tribological behavior of chromized AISI 52100 steel showed that the wear and friction decrease with increasing contact loads. Higher contact pressures enable the formation of a Cr_2O_3 layer, which provides a lubricated contact and essentially enhances tribological performance. The chromized layer consisted of an outermost layer of Cr_7C_3 grains and an inner layer of coarse Fe_3C grains [105].

Any relevant reviewed literature on tribocorrosion of chromized steels examined medium-carbon C45 steel; however, the studies did not provide a mechanistic explanation. Tribological testing of case-chromized C45 steel in salt water showed better tribocorrosion resistance than the untreated one [109]. Another study compared the tribological performance of heat-treated and non-heat-treated case-chromosiliconized C45 steel. Chromosiliconized layers improved wear resistance in a sugar slurry environment. At higher contact loads, wear exceeded layer thickness, causing frictional seizure [108].

The high-temperature chromizing treatment can alter the morphology and properties of the steel material near the chromized layer [118,119]. High-temperature chromizing was shown to reduce the bulk hardness of the M300 maraging steel due to grain coarsening [110]. Grain coarsening can be prevented by reducing the process temperature, which could reduce the thickness of the

Table 7 Summary of the literature on microstructure and properties of case-hardened steels reviewed in this article

Case-hardening method	Carburizing	Boriding	Nitriding	Nitrocarburizing	Carbonitriding	Chromizing
Layer microstructure	Carbon-rich martensite with retained austenite, bainite, pearlite, or ferrite [35]	Fe_2B or Fe_2B/FeB [19,28,50]	ε and γ' iron nitride [36]	ε and γ' iron nitride [36]	Martensitic or bainitic with nitrides and carbides [90,94]	$M_{23}C_6$ M_7C_3 [101–103]
Compound layer thickness (μm)	–	50–250 [19]	10–25 [36]	10–25 [36]	–	15–125 [23]
Diffused zone thickness (μm)	50–1500 [36]	<250 [19]	75–750 [21,26]	<200 [26]	75–750 [95]	<150 [102,107]
Hardness (HV)	650–970 [18]	700–3370 [19]	890–1700 [1]	700–1200 (this review)	<850 [1]	1400–1900 (this review)
Process temperature (°)	880–1050 [36]	800–1000 [19]	500–580 [36]	495–775 [36,112]	775–900 [95]	800–1300 [23]
Applicable steels	Low carbon 0.1–0.25% Low-carbon alloy-bearing steels [1]	Alloy steel, tool steel, and Co and Ni alloys [19,112]	Medium carbon, AISI low- and high-alloy steels containing Al, Cr, V, and Mo, stainless steels [112]	Medium- and high-carbon steels, alloy steels [1]	Low-carbon alloy steels, stainless steels [1,95]	Low-carbon-bearing steels [112]

chromized layer. However, Wang et al. [111] showed that refining the grains in the surface layer of low-carbon steel promoted diffusion of chromium.

Although the literature provides limited studies on the tribological and tribocorrosion behavior of chromized steels, existing research has demonstrated that chromizing enhances their wear and tribocorrosion resistance. The thickness and quality of the chromized layer can be influenced by the process parameters and composition of the base metal. In general, low-carbon content of the base metal tends to produce thicker chromized layers [23]; however, Lee and Duh [101] reported contradicting results in which chromizing of high-carbon 1095 steel resulted in a thicker layer than in low-carbon 1020 steel. By contrast, higher carbon content favors the formation of Cr_3C_2, which enhances the hardness and wear resistance. Nevertheless, the reviewed studies showed that longer chromizing durations and higher temperatures yield thicker layers, which improved the wear resistance. High-alloy steels such as tool steels form thinner layers because alloying elements such as chromium, molybdenum, and tungsten tend to slow the diffusion. As a result, high-alloy steels with high hardness and wear resistance may not benefit from chromizing to such an extent as carbon steels.

4 Comparison of Case-Hardening Methods

A comparison of microstructure, layer thickness, hardness, process temperature, tribological and tribocorrosion performance, and applicable steel materials of the reviewed case-hardening methods is summarized in Table 7. As shown in this review, these properties and performance depend on the process parameters and steel composition, but a general comparison can be made. Hard compound layers are formed with boriding, nitriding, nitrocarburizing, and chromizing surface treatments. Although carburizing and carbonitriding typically form only a diffused layer, carbonitriding can also produce a very thin compound layer. Nitrided and carbonitrided compound layers are much thinner than the borided and chromized layers. The presence of compound layers increases the hardness. Boriding provides the highest hardness among all the case-hardening methods reviewed. Carburizing and carbonitriding result in the lowest hardness, but they achieve the deepest case depth. Most of the reviewed literature demonstrates that the increase in the hardness and thickness of the case-hardened layer can improve wear resistance. These results suggest that boriding, nitriding, nitrocarburizing, and chromizing should provide superior wear performance compared with carburizing and carbonitriding methods. To determine the relative wear performance of the case-hardening methods, they need to be compared directly. However, only a few studies have directly compared different case-hardening methods. A study comparing boriding, carburizing, and carbonitriding of AISI 1020 and 5110 demonstrated that boriding resulted in the highest hardness, thereby achieving the lowest wear and friction. By contrast, the softest carburized steel achieved the highest wear and friction [25]. Boriding surface treatment also outperformed nitrocarburizing treatment on AISI 4130 [5]. In a study examining M50NiL steel, nitriding after carburizing resulted in higher wear resistance and lower friction compared with carburizing alone [100].

Carburizing and nitriding are two commonly applied methods to enhance the tribocorrosion resistance of steel. Like tribological performance, the tribocorrosion performance of case-hardening methods needs to be directly compared for evaluation. A comparative study was conducted on the tribocorrosion behavior of low-temperature nitrided and carburized 316L stainless steel in 0.5 M H_2SO_4 solution [45]. In dry sliding wear tests, both treated steels showed higher wear resistance and effectively reduced adhesive wear compared with untreated steel. Specifically, the nitrided layer, despite being thinner, outperformed the carburized layer because of its higher hardness. However, in tribocorrosion testing under open circuit potential conditions, the carburized layer improved the tribocorrosion resistance of 316L stainless steel by 40% by providing high resistance to mechanical wear and great passivity against corrosion. By contrast, the nitrided layer exhibited worse performance than the untreated steel because of the combined effects of metal dissolution and mechanical wear. This result suggests that low-temperature nitriding is not suitable for increasing the tribocorrosion resistance of 316 stainless steel in H_2SO_4 environments. The passivation mechanisms of carburizing and nitriding, as observed in stainless steel systems [47,81], show some distinct behaviors. A high-carbon concentration in the carburized layer slows passive film growth compared with the untreated layer. However, the passive film continues to improve over time, reducing corrosion and minimizing the risk of galvanic coupling under tribocorrosion conditions. On the other hand, high nitrogen concentrations may negatively affect corrosion resistance due to the presence of precipitates, whereas lower nitrogen levels enhance passivation by promoting anodic dissolution, corrosion products formation, and the accumulation of nitrides. Thus, the selection of case-hardening methods for improving tribocorrosion resistance should be tailored to specific steel materials and service environments.

Although the primary purpose of the case-hardening is to enhance surface hardness, wear resistance, and in some cases, corrosion resistance, it is important to consider the potential impact of the high-temperature processes on the bulk properties of the treated steel materials. Among the case-hardening techniques reviewed, nitriding and nitrocarburizing offer the advantage of being low-temperature processes. As a result, they are less likely to alter the microstructural, morphological, or mechanical properties of the bulk material, making them more suitable for materials and applications that are sensitive to higher temperature exposures.

5 Summary

Several conclusions can be drawn based on the literature review of the tribological and tribocorrosion characterization of case-hardened steels. The six case-hardening methods—boriding, chromizing, carburizing, nitriding, nitrocarburizing, and carbonitriding—all increase the hardness and wear resistance of steels compared with the untreated counterparts. The tribological behavior is affected by the microstructure and composition of the case-hardened layer, which depends on the process parameters and steel composition. The thickness of the case-hardened layer tends to increase with a higher process temperature and/or a longer duration. The hardness of the layer can be increased by a higher compound concentration. In most cases, higher hardness leads to improved wear resistance, but it may also cause brittle failures such as spalling or delamination, compromising the wear performance. Although alloying elements such as tungsten, molybdenum, and chromium contained in the steel promote the formation of carbides in the case-hardened layer, they also decrease the diffusion rate of the compound into the substrate, thereby yielding a thinner layer. Case-hardening seems to have an inconsistent effect on friction behavior, varying from case to case without an apparent trend. Case-hardening also affects the tribocorrosion resistance of steels. Designing case-hardening techniques tailored to the specific application environment with a strong interface bonding is crucial for effective wear and tribocorrosion protection.

Acknowledgment

The research was sponsored by the Feedstock-Conversion Interface Consortium of the Bioenergy Technologies Office, Office of Energy Efficiency and Renewable Energy, US Department of Energy. This manuscript has been authored by UT-Battelle, LLC, under contract DE-AC05-00OR22725 with the U.S. Department of Energy (DOE). DOE will provide public access to these results of federally sponsored research in accordance with the DOE Public Access Plan Access Plan.[2]

Conflict of Interest

There are no conflicts of interest.

Data Availability Statement

No data, models, or code were generated or used for this article.

References

[1] Schneider, M. J., and Chatterjee, M. S., 2013, "Introduction to Surface Hardening of Steels," *Steel Heat Treating Fundamentals and Processes*, J. L. Dossett, and G. E. Totten, eds., ASM Handbook, ASM International, OH, pp. 389–398.

[2] Davis, J. R., 2002, *Surface Hardening of Steels: Understanding the Basics*, ASM International, OH.

[3] Kishawy, H. A., and Hosseini, A., 2018, *Materials Forming, Machining and Tribology: Machining Difficult-to-Cut Materials Basic Principles and Challenges*, Springer, Switzerland.

[4] Genel, K., Demirkol, M., and Gülmez, T., 2000, "Corrosion Fatigue Behaviour of Ion Nitrided AISI 4140 Steel," Mater. Sci. Eng. A, **288**(1), pp. 91–100.

[5] Nora, R., Zine, T. M., Abdelkader, K., Youcef, K., Ali, O., and Jiang, X., 2019, "Boriding and Boronitrocarburising Effects on Hardness, Wear and Corrosion Behavior of AISI 4130 Steel," Rev. Mater., **24**(1), pp. 1–9.

[6] Sezgin, C. T., and Hayat, F., 2022, "The Effects of Boriding Process on Tribological Properties and Corrosive Behavior of a Novel High Manganese Steel," J. Mater. Process. Technol., **300**, p. 117421.

[7] Li, C. X., and Bell, T., 2006, "Corrosion Properties of Plasma Nitrided AISI 410 Martensitic Stainless Steel in 3.5% NaCl and 1% HCl Aqueous Solutions," Corros. Sci., **48**(8), pp. 2036–2049.

[8] Sola, R., Poli, G., Veronesi, P., and Giovanardi, R., 2014, "Effects of Surface Morphology on the Wear and Corrosion Resistance of Post-Treated Nitrided and Nitrocarburized 42CrMo4 Steel," Metall. Mater. Trans. A, **45**(6), pp. 2827–2833.

[9] Petrova, R. S., Suwattananont, N., and Samardzic, V., 2008, "The Effect of Boronizing on Metallic Alloys for Automotive Applications," J. Mater. Eng. Perform., **17**(3), pp. 340–345.

[10] Emun, B. Y., 2019, "Corrosion Evaluation of Chromized Steel Utilized in Automotive Exhaust Applications," Ph.D. dissertation, McMaster University, Hamilton, ON.

[11] Hernández-Sánchez, E., Hernández-Domínguez, D., Tadeo-Rosas, R., Sánchez-Fuentes, Y., Linares-Duarte, L. A., Orozco-Álvarez, C., Miranda-Hernández, J. G., and Carrera-Espinoza, R., 2024, "Tribological and Mechanical Behavior of Automotive Crankshaft Steel Superficially Modified Using the Boriding Hardening Process," Coatings, **14**(6), p. 716.

[12] Streit, E., and Trojahn, W., 2002, "Duplex Hardening of Aerospace Bearings," *Bearing Steel Technology*, J. M. Beswick, ed., ASTM, Philadelphia, PA, pp. 386–398.

[13] Gloeckner, P., and Rodway, C., 2017, "The Evolution of Reliability and Efficiency of Aerospace Bearing Systems," Engineering, **9**(11), pp. 962–991.

[14] Metel, A., Grigoriev, S., Melnik, Y., Panin, V., and Prudnikov, V., 2011, "Cutting Tools Nitriding in Plasma Produced by a Fast Neutral Molecule Beam," Jpn. J. Appl. Phys., **50**(8S1), p. 08JG04.

[15] Grejtak, T., Lacey, J. A., Kuns, M. W., Hartley, D. S., Thompson, D. N., Fenske, G., Ajayi, O. O., and Qu, J., 2023, "Improving Knife Milling Performance for Biomass Preprocessing by Using Advanced Blade Materials," Wear, **522**, p. 204714.

[16] Wołowiec-Korecka, E., 2024, *Carburising and Nitriding of Iron Alloys*, Springer Nature, Switzerland.

[17] Vamshi, M., Singh, S. K., Sateesh, N., Nagaraju, D. S., and Subbiah, R., 2019, "A Review on Influence of Carburizing on Ferritic Stainless Steel," Mater. Today: Proc., **26**, pp. 937–943.

[18] Fuller, A. J. Jr, 2013, "Introduction to Carburising and Carbonitriding," *Steel Heat Treating Fundamentals and Processes*, Vol. 4A, J. L. Dossett, and G. E. Totten, eds., ASM Handbook, ASM International, Almere, The Netherlands, pp. 505–521.

[19] Zimmerman, C., 2013, "Boriding (Boronizing) of Metals," *Steel Heat Treating Fundamentals and Processes*, Vol. 4A, J. L. Dossett, and G. E. Totten, eds., ASM Handbook, ASM International, Materials Park, OH, pp. 709–724.

[20] Wang, B., Liu, B., Gu, J., and Somers, M. A. J., 2022, "Gaseous Carbonitriding of High Carbon Chromium Bearing Steel: Correlation Between Composition, Microstructure and Stability," Surf. Coat. Technol., **438**, p. 128408.

[21] Senatorski, J., Tacikowski, J., Rolinski, E., and Lampman, S., 2017, "Tribology of Nitrided and Nitrocarburized Steels," *ASM Handbook: Friction, Lubrication and Wear Technology*, Vol. 18, G. Totten, ed., ASM International, Novelty, OH, pp. 638–652.

[22] Nie, X., Tsotsos, C., Wilson, A., Yerokhin, A. L., Leyland, A., and Matthews, A., 2001, "Characteristics of a Plasma Electrolytic Nitrocarburising Treatment for Stainless Steels," Surf. Coat. Technol., **139**(2–3), pp. 135–142.

[23] Castle, A. R., and Gabe, D. R., 1999, "Chromium Diffusion Coatings," Int. Mater. Rev., **44**(2), pp. 37–58.

[24] Meier, G. H., Cheng, C., Perkins, R. A., and Bakker, W., 1989, "Diffusion Chromizing of Ferrous Alloys," Surf. Coat. Technol., **39–40**, pp. 53–64.

[25] Selçuk, B., Ipek, R., and Karamış, M. B., 2003, "A Study on Friction and Wear Behaviour of Carburized, Carbonitrided and Borided AISI 1020 and 5115 Steels," J. Mater. Process. Technol., **141**(2), pp. 189–196.

[26] Czerwinski, F., 2012, "Thermochemical Treatment of Metals," *Heat Treatment—Conventional and Novel Applications*, F. Czerwinski, ed., Intech, pp. 73–102.

[27] Grejtak, T., and Qu, J., 2023, "Improving Mechanical Properties of Carbon and Tool Steels via Chromizing," Adv. Appl. Ceram., **122**(3–4), pp. 215–225.

[28] Zimmerman, C., 2017, "Wear and Galling Resistance of Borided (Boronized) Metal Surfaces," *ASM Handbook: Friction, Lubrication, and Wear Technology*, Vol. 18, G. E. Totten, ed., ASM International, Novelty, OH, pp. 653–660.

[29] Izciler, M., and Tabur, M., 2006, "Abrasive Wear Behavior of Different Case Depth Gas Carburized AISI 8620 Gear Steel," Wear, **260**(1–2), pp. 90–98.

[30] Wołowiec-Korecka, E., 2023, "Case Hardening Development Review (2001–2020)," Arch. Mater. Sci. Eng., **120**(2), pp. 70–85.

[31] Bhushan, B., and Ko, P. L., 2003, *Introduction to Tribology*, Wiley, NY.

[32] Totten, G. E., 2017, *Friction, Lubrication, and Wear Technology*, ASM International, OH.

[2] http://energy.gov/downloads/doe-public-access-plan

[33] McGuire, M. F., 2008, *Stainless Steels for Design Engineers*, ASM International, OH.

[34] Mesquita, R. A., 2016, *Tool Steels: Properties and Performance*, CRC Press, Boca Raton, FL.

[35] Krauss, G., 2014, "Microstructures and Properties of Carburized Steels," *Heat Treating of Irons and Steels*, ASM International, pp. 76–87.

[36] Mittemeijer, E. J., and Somers, M. A. J., 2015, *Thermochemical Surface Engineering of Steels*, Woodhead Publishing, Cambridge.

[37] Boumediri, H., Touati, S., Debbah, Y., Selami, S., Chitour, M., Khelifa, M., Kahaleras, M. S., et al., 2024, "Effect of Carburizing Time Treatment on Microstructure and Mechanical Properties of Low Alloy Gear Steels," Mater. Res. Express, **11**(7), p. 076505.

[38] Zhu, Z., Liang, Y., Yin, C., Ren, X., Yang, M., and Zou, J., 2022, "Influence of Friction-Induced Retained Austenite Transformation to Martensite on the Wear Properties of a Carburized Layer of 23CrNi3MoA Steel," Appl. Surf. Sci., **595**, p. 153548.

[39] Roy, S., and Sundararajan, S., 2016, "The Effect of Heat Treatment Routes on the Retained Austenite and Tribomechanical Properties of Carburized AISI 8620 Steel," Surf. Coat. Technol., **308**, pp. 236–243.

[40] Zhang, P., Zhang, F. C., Yan, Z. G., Wang, T. S., and Qian, L. H., 2011, "Wear Property of Low-Temperature Bainite in the Surface Layer of a Carburized Low Carbon Steel," Wear, **271**(5–6), pp. 697–704.

[41] Tang, J., Hu, X., Lai, F., Guo, X., Qu, S., He, R., Qin, S., and Li, J., 2020, "Evolution of Fretting Wear Behaviors and Mechanisms of 20CrMnTi Steel After Carburizing," Metals (Basel), **10**(2), p. 179.

[42] Shi, L., Cui, X., Li, J., Jin, G., Liu, J., and Tian, H., 2022, "Improving the Wear Resistance of Heavy-Duty Gear Steels by Cyclic Carburizing," Tribol. Int., **171**, p. 107576.

[43] Thirugnanasambantham, K. G., and Ganesh Kumar, A. G., 2018, "Mechanistic Studies on Degradation in Sliding Wear Behavior of Carburized AISI 8620 Steel at 10 °C Under Unlubricated Conditions," Materials Today: Proceedings, **5**(2), pp. 6258–6267.

[44] Sun, Y., and Haruman, E., 2011, "Effect of Electrochemical Potential on Tribocorrosion Behavior of Low Temperature Plasma Carburized 316L Stainless Steel in 1M H_2SO_4 Solution," Surf. Coat. Technol., **205**(17–18), pp. 4280–4290.

[45] Sun, Y., and Bailey, R., 2023, "Comparison of Wear Performance of Low Temperature Nitrided and Carburized 316L Stainless Steel Under Dry Sliding and Corrosive-Wear Conditions," J. Mater. Eng. Perform., **32**(3), pp. 1238–1247.

[46] Mainardi, V. A., Cardoso, R. P., Brunatto, S. F., and Scheuer, C. J., 2024, "Tribocorrosion Behavior of Low-Temperature Plasma-Carburized AISI 420 Martensitic Stainless Steel: Investigating the Synergy Between Corrosion and Erosion in Slurry and Liquid Impingement Environments," Surf. Coat. Technol., **477**, p. 130373.

[47] Niu, W., Lillard, R. S., Li, Z., and Ernst, F., 2015, "Properties of the Passive Film Formed on Interstitially Hardened AISI 316L Stainless Steel," Electrochim. Acta, **176**, pp. 410–419.

[48] Zhang, R., Yuan, Q., Tang, E., Mo, J., Zhang, Z., Hu, H., and Xu, G., 2023, "Role of Precipitates on the Grain Coarsening of 20CrMnTi Gear Steel During Pseudo-Carburizing," Metals (Basel), **13**(8), p. 1422.

[49] Dybowski, K., and Klimek, L., 2023, "Identification of Intermetallic Phases Limiting the Growth of Austenite Grains in the Low-Pressure Carburizing Process," Crystals (Basel), **13**(12), p. 1683.

[50] Zimmermann, C., and Bugliarello-Wondrich, N., 2014, "Deep Case Boriding for Extreme Wear Resistance," AM&P Tech. Art., **172**(11), pp. 41–44.

[51] Tsipas, D. N., and Rus, J., 1987, "Boronizing of Alloy Steels," J. Mater. Sci. Lett., **6**(1), pp. 118–120.

[52] Campos-Silva, I., Ortiz-Domínguez, M., Tapia-Quintero, C., Rodríguez-Castro, G., Jiménez-Reyes, M. Y., and Chávez-Gutiérrez, E., 2012, "Kinetics and Boron Diffusion in the FeB/Fe_2B Layers Formed at the Surface of Borided High-Alloy Steel," J. Mater. Eng. Perform., **21**(8), pp. 1714–1723.

[53] Vinodh Kumar, S., Surya Raj, G., and Prince, M., 2022, "Effects of Pack Boriding and Induction Boriding on the Dry Sliding Wear Behavior of High Speed Steel," Mater. Today: Proc., **59**, pp. 1105–1110.

[54] Türkmen, İ, Yalamaç, E., and Keddam, M., 2019, "Investigation of Tribological Behaviour and Diffusion Model of Fe_2B Layer Formed by Pack-Boriding on SAE 1020 Steel," Surf. Coat. Technol., **377**, p. 124888.

[55] Motallebzadeh, A., Dilektasli, E., Baydogan, M., Atar, E., and Cimenoglu, H., 2015, "Evaluation of the Effect of Boride Layer Structure on the High Temperature Wear Behavior of Borided Steels," Wear, **328–329**, pp. 110–114.

[56] Gök, M. S., Küçük, Y., Erdoğan, A., Öge, M., Kanca, E., and Günen, A., 2017, "Dry Sliding Wear Behavior of Borided Hot-Work Tool Steel at Elevated Temperatures," Surf. Coat. Technol., **328**, pp. 54–62.

[57] Erdogan, A., 2019, "Boriding Temperature Effect on Micro-Abrasion Wear Resistance of Borided Tool Steel," ASME J. Tribol, **141**(12), p. 121603.

[58] Yapici, A., Aydin, S. E., Koc, V., Kanca, E., and Yildiz, M., 2019, "Wear Behavior of Borided AISI D2 Steel Under Linear Reciprocating Sliding Conditions," Prot. Met. Phys. Chem. Surf., **55**(2), pp. 341–351.

[59] Arteaga-Hernandez, L. A., Cuao-Moreu, C. A., Gonzalez-Rivera, C. E., Alvarez-Vera, M., Ortega-Saenz, J. A., and Hernandez-Rodriguez, M. A. L., 2021, "Study of Boriding Surface Treatment in the Tribological Behavior of an AISI 316L Stainless Steel," Wear, **477**, p. 203825.

[60] Grejtak, T., Kuns, M. W., Lacey, J. A., Ajayi, O. O., Fenske, G., Blau, P. J., and Qu, J., 2025, "Enhancing the Shredder Durability for Biomass Preprocessing by Utilizing Wear-Resistant Cutter Materials," Tribol. Int., **210**, p. 110766.

[61] Greco, A., Mistry, K., Sista, V., Eryilmaz, O., and Erdemir, A., 2011, "Friction and Wear Behaviour of Boron Based Surface Treatment and Nano-Particle Lubricant Additives for Wind Turbine Gearbox Applications," Wear, **271**(9–10), pp. 1754–1760.

[62] Morón, R. C., Hernández-Onofre, I., Contla-Pacheco, A. D., Bravo-Bárcenas, D., and Campos-Silva, I., 2020, "Friction and Reciprocating Wear Behavior of Borided AISI H13 Steel Under Dry and Lubricated Conditions," J. Mater. Eng. Perform., **29**(7), pp. 4529–4540.

[63] Morón, R. C., Arellano-Ortiz, G. A., Rodríguez-Castro, G. A., Meneses-Amador, A., Cruz-Ramírez, A., Méndez-Méndez, J. V., and Campos-Silva, I., 2021, "Wear Performance Under Dry and Lubricated Conditions of Post Boriding Heat Treatment in 4140 Steel," ASME J. Tribol., **143**(2), p. 021601.

[64] da Costa Aichholz, S. A., Sostag Meruvia, M., Soares Júnior, P. C., and Torres, R. D., 2018, "Tribocorrosion Behavior of Boronized AISI 4140 Steel," Surf. Coat. Technol., **352**, pp. 265–272.

[65] Campos-Silva, I., Palomar-Pardavé, M., Pastén-Borja, R. P., Feridun, O. K., Bravo-Bárcena, D., López-García, C., and Reyes-Helguera, R., 2018, "Tribocorrosion and Cytotoxicity of FeB–Fe_2B Layers on AISI 316L Steel," Surf. Coat. Technol., **349**, pp. 986–997.

[66] Liapina, T., Leineweber, A., and Mittemeijer, E. J., 2003, "Nitrogen Redistribution in ε/γ'-Iron Nitride Compound Layers Upon Annealing," Scr. Mater., **48**(12), pp. 1643–1648.

[67] Podgornik, B., Vižintin, J., Wänstrand, O., Larsson, M., Hogmark, S., Ronkainen, H., and Holmberg, K., 2001, "Tribological Properties of Plasma Nitrided and Hard Coated AISI 4140 Steel," Wear, **249**(3–4), pp. 254–259.

[68] Pala, Z., Mušálek, R., Kyncl, J., Harcuba, P., Stráský, J., Kolařík, K., Ganev, N., and Matějíček, J., 2014, "Effect of Boriding Time on Microstructure and Residual Stresses in Borided Highly Alloyed X210CR12 Steel," Key Eng. Mater., **606**, pp. 27–30.

[69] Bhaskar, S. V., and Kudal, H. N., 2017, "Tribology of Nitrided-Coated Steel—A Review," Arch. Mech. Technol. Mater., **37**(1), pp. 50–57.

[70] Yan, M. F., Chen, B. F., and Li, B., 2018, "Microstructure and Mechanical Properties From an Attractive Combination of Plasma Nitriding and Secondary Hardening of M50 Steel," Appl. Surf. Sci., **455**, pp. 1–7.

[71] Wang, Z. W., Li, Y., Zhang, Z. H., Zhang, S. Z., Ren, P., Qiu, J. X., Wang, W. W., Bi, Y. J., and He, Y. Y., 2021, "Friction and Wear Behavior of Duplex-Treated AISI 316L Steels by Rapid Plasma Nitriding and (CrWAlTiSi)N Ceramic Coating," Results Phys., **24**, p. 104132.

[72] Karamiş, M. B., 1991, "An Investigation of the Properties and Wear Behaviour of Plasma-Nitrided Hot-Working Steel (H13)," Wear, **150**(1–2), pp. 331–342.

[73] Miyamoto, J., and Abraha, P., 2019, "The Effect of Plasma Nitriding Treatment Time on the Tribological Properties of the AISI H13 Tool Steel," Surf. Coat. Technol., **375**, pp. 15–21.

[74] Menthe, E., Bulak, A., Olfe, J., Zimmermann, A., and Rie, K.-T., 2000, "Improvement of the Mechanical Properties of Austenitic Stainless Steel After Plasma Nitriding," Surf. Coat. Technol., **133–134**, pp. 259–263.

[75] Yilbas, B. S., and Nizam, S. M., 2000, "Wear Behavior of TiN Coated AISI H11 and AISI M7 Twist Drills Prior to Plasma Nitriding," J. Mater. Process. Technol., **105**(3), pp. 352–358.

[76] Chen, W., Xia, M., and Song, W., 2020, "Study on the Anti-Friction Mechanism of Nitriding Surface Texture 304 Steel," Coatings, **10**(6), p. 554.

[77] Possoli, F. A. A., Souza, A. P. N., Bernardelli, E. A., and Borges, P. C., 2024, "Tribocorrosion Assessment of Low-Temperature Plasma Nitrided Super Duplex Stainless Steel," Surf. Coat. Technol., **479**, p. 130572.

[78] Haruman, E., Sun, Y., and Adenan, M. S., 2020, "A Comparative Study of the Tribocorrosion Behaviour of Low Temperature Nitrided Austenitic and Duplex Stainless Steels in NaCl Solution," Tribol. Int., **151**, p. 106412.

[79] Sun, Y., and Bailey, R., 2023, "Tribocorrosion Behavior of γ'-Fe_4N Nitride Layer Formed on Mild Steel by Plasma Nitriding in Chloride-Containing Solution," Lubricants, **11**(7), p. 281.

[80] Boztepe, E., Alves, A. C., Ariza, E., Rocha, L. A., Cansever, N., and Toptan, F., 2018, "A Comparative Investigation of the Corrosion and Tribocorrosion Behaviour of Nitrocarburized, Gas Nitrided, Fluidized-Bed Nitrided, and Plasma Nitrided Plastic Mould Steel," Surf. Coat. Technol., **334**, pp. 116–123.

[81] Kuczynska-Wydorska, M., and Flis, J., 2008, "Corrosion and Passivation of Low-Temperature Nitrided AISI 304L and 316L Stainless Steels in Acidified Sodium Sulphate Solution," Corros. Sci., **50**(2), pp. 523–533.

[82] Karamiş, M. B., 1991, "Tribological Behaviour of Plasma Nitrided 722M24 Material Under Dry Sliding Conditions," Wear, **147**(2), pp. 385–399.

[83] Pye, D., 2003, *Practical Nitriding and Ferritic Nitrocarburizing*, ASM International, OH.

[84] Du, H., Somers, M. A. J., and Agren, J., 2000, "Microstructural and Compositional Evolution of Compound Layers During Gaseous Nitrocarburizing," Metall. Mater. Trans. A, **31**(1), pp. 195–211.

[85] Zhang, C. S., Yan, M. F., Sun, Z., Wang, Y. X., You, Y., Bai, B., Chen, L., Long, Z., and Li, R. W., 2014, "Optimizing the Mechanical Properties of M50NiL Steel by Plasma Nitrocarburizing," Appl. Surf. Sci., **315**(1), pp. 28–35.

[86] Wen, D. C., 2010, "Erosion and Wear Behavior of Nitrocarburized DC53 Tool Steel," Wear, **268**(3–4), pp. 629–636.

[87] Karamboiki, C. M., Mourlas, A., Psyllaki, P., and Sideris, J., 2013, "Influence of Microstructure on the Sliding Wear Behavior of Nitrocarburized Tool Steels," Wear, **303**(1–2), pp. 560–568.

[88] Jeyakymar, M., Munusami, V., Shanmugam, P., Boopalan, N., Boopathi, S., and Sureshkumar, M., 2022, "An Investigation on Wear Loss and Hardness of Nitro-Carburizing Coated Stainless-Steel Grade-316," Mater. Today: Proc., **66**, pp. 1398–1404.

[89] Heydarzadeh Sohi, M., Ebrahimi, M., Honarbakhsh Raouf, A., and Mahboubi, F., 2010, "Effect of Plasma Nitrocarburizing Temperature on the Wear Behavior of AISI 4140 Steel," Surf. Coat. Technol., **205**, pp. 1711–1717.
[90] Liu, R. L., Yi, B., Li, Z., and Liu, Q. L., 2025, "Surface Hardening of AISI 431 Stainless Steel by Plasma Electrolytic Carbonitriding Without Sacrificing Its Corrosion Resistance," Surf. Interfaces, **62**, p. 106216.
[91] Fazlalipour, F., Shakib, N., Shokuhfar, A., and Niki Nushari, M., 2012, "Effect of Nitro-Carburizing Treatment on Wear Mechanism and Friction of Steel/WC-Co Sliding Couple," ASME J. Tribol., **134**(1), p. 011401.
[92] Chen, R., Chen, H., Ye, C., Li, F., Miao, Y., Zhao, Y., Sun, X., and Zhao, Z., 2024, "Friction, Wear, and Corrosion Behavior of Nitrocarburized HT250 Gray Cast Iron," Int. J. Electrochem. Sci., **19**(6), p. 100582.
[93] Herring, D. H., 2011, "Carbonitriding of Fasteners," Fasten. Technol. Int., **34**, pp. 52–54.
[94] Liu, B., Wang, B., and Gu, J., 2019, "Effect of Ammonia Addition on Microstructure and Wear Performance of Carbonitrided High Carbon Bearing Steel AISI 52100," Surf. Coat. Technol., **361**, pp. 112–118.
[95] Dossett, J., 2013, "Carbonitriding of Steels," *Steel Heat Treating Fundamentals and Processes*, J. L. Dossett, and G. E. Totten, eds., ASM Handbook, ASM International, OH, pp. 599–616.
[96] Liu, J., Dong, H., Buhagiar, J., Song, C. F., Yu, B. J., Qian, L. M., and Zhou, Z. R., 2011, "Effect of Low-Temperature Plasma Carbonitriding on the Fretting Behaviour of 316LVM Medical Grade Austenitic Stainless Steels," Wear, **271**(9–10), pp. 1490–1496.
[97] Li, Q., Xiao, K., Lu, Z., Shi, Y., Lin, W., and Zhang, S., 2024, "Mechanism of Laser Carbonitriding Enhancing the Wear Resistance of 45# Steel," Mater. Today Commun., **38**, p. 108327.
[98] El-Rahman, A. M. A., 2010, "An Investigation on the Microstructure, Tribological and Corrosion Performance of AISI 321 Stainless Steel Carbonitrided by RF Plasma Process," Surf. Coat. Technol., **205**(2), pp. 674–681.
[99] Chongyang, N., Tianlin, Z., Yue, X., Lixia, Y., and Guixiang, W., 2022, "Study on Preparation and Friction Characteristics of Steel 1045 Modified Layer Based on Plasma Electrolytic Carbonitriding," Mater. Today Commun., **33**, p. 104518.
[100] Zeng, G., Liang, Y., Li, S., Sun, Y., and Wang, P., 2024, "Effect of Carbonitride on the Friction and Wear Properties of M50NiL Steel After Sequential Carburizing and Nitriding Treatment," Mater. Today Commun., **41**, p. 110251.
[101] Lee, J. W., and Duh, J. G., 2004, "Evaluation of Microstructures and Mechanical Properties of Chromized Steels With Different Carbon Contents," Surf. Coat. Technol., **177–178**, pp. 525–531.
[102] Glowacki, Z., and Kaluba, W., 1982, "On Some Features of Chromium Carbide Diffusion Layer Formation," Metall. Trans. A, **13**(5), pp. 753–759.
[103] Zancheva, L., Hillert, M., Lange, N., Seetharaman, S., and Staffansson, L.-I., 1978, "On the Formation of Carbide Coatings by Chromizing Carbon Steels," Metall. Trans. A, **9**(7), pp. 909–915.
[104] Lee, J. W., Wang, H. C., Li, J. L., and Lin, C. C., 2004, "Tribological Properties Evaluation of AISI 1095 Steel Chromized at Different Temperatures," Surf. Coat. Technol., **188–189**(1–3 SPEC.ISS.), pp. 550–555.
[105] Tan, C., Zong, X., Zhou, W., Cao, H., Wang, J., Wang, C., Peng, J., et al., 2022, "Insights Into the Microstructure Characteristics, Mechanical Properties and Tribological Behaviour of Gas-Phase Chromized Coating on GCr15 Bearing Steel," Surf. Coat. Technol., **443**, p. 128605.
[106] Wang, X., Zhang, R., Zhou, T., Wei, X., Liaw, P., Feng, R., Wang, W., and Li, R., 2018, "Microstructural Evolution in Chroming Coatings Friction Pairs Under Dry Sliding Test Conditions," Adv. Tribol., **2018**, p. 5962153.
[107] Li, S., Yang, Z., Wan, Q., Hou, J., Xiao, Y., Zhang, X., Gao, R., and Meng, L., 2022, "Increase in Wear Resistance of Traction Wheel via Chromizing: A Study Combining Experiments and Simulations," Coatings, **12**(9), p. 1275.
[108] Bauer, I., and Baryga, A., 2013, "Tribocorrosion of a chromosiliconized layer," Technical Sciences/University of Warmia and Mazury in Olsztyn.
[109] Kasprzycka, E., Senatorski, J., Nakonieczny, A., and Babul, T., 2003, "Diffusion Layers Produced on Carbon Steel Surface by Means of Vacuum Chromizing Process," J. Mater. Eng. Perform., **12**(6), pp. 693–695.
[110] Funch, C. V., Dahl, K. V., Christiansen, T. L., and Somers, M. A. J., 2022, "Chromizing of Additively Manufactured Maraging Steel; Microstructural Evolution and Corrosion Performance," HTM J. Heat Treat. Mater., **77**(4), pp. 245–268.
[111] Wang, Z. B., Lu, J., and Lu, K., 2005, "Chromizing Behaviors of a Low Carbon Steel Processed by Means of Surface Mechanical Attrition Treatment," Acta Mater., **53**(7), pp. 2081–2089.
[112] Dossett, J. L., and Totten, G. E., 2013, *Steel Heat Treating Fundamentals and Processes*, ASM International, Materials Park, OH.
[113] Łukaszewicz, G., Tacikowski, M., Kulka, M., Chmielarz, K., and Świątnicki, W. A., 2023, "The Effect of Hybrid Treatment Combining Boriding and Nanobainitising on the Tribological and Mechanical Properties of 66SiMnCrMo6-6-4 Bearing Steel," Materials, **16**(9), p. 3436.
[114] Gao, Y., Xue, X., and Yang, H., 2015, "Influence of Boron on Initial Austenite Grain Size and Hot Deformation Behavior of Boron Microalloyed Steels," Crystals (Basel), **5**(4), pp. 592–607.